Geomorphology 388 (2021) 107781

Contents lists available at ScienceDirect

Geomorphology

journal homepage: www.elsevier.com/locate/geomorph

Penultimate Glacial Cycle glacier extent in the Iberian Peninsula: New evidence from the Serra da Estrela (Central System, Portugal)

Gonçalo Vieira [a,*], David Palacios [b], Nuria Andrés [b], Carla Mora [a], Lorenzo Vázquez Selem [c], Barbara Woronko [d], Carmen Soncco [a], Jose Úbeda [b], Gabriel Goyanes [e]

[a] Centre of Geographical Studies, Institute of Geography and Spatial Planning, University of Lisbon, Rua Branca Edmée Marques, 1600-276 Lisboa, Portugal
[b] High Mountain Physical Geography Research Group, Department of Geography, Universidad Complutense de Madrid, 28040 Madrid, Spain.
[c] Institute of Geography, Universidad Nacional Autónoma de México, México DF, Mexico
[d] Faculty of Geology, University of Warsaw, Żwirki i Wigury 92, 02-089 Warsaw, Poland
[e] Centre of Natural Resources and Environment, Instituto Superior Técnico, University of Lisbon, Portugal

ARTICLE INFO

Article history:
Received 14 April 2021
Received in revised form 10 May 2021
Accepted 11 May 2021
Available online 14 May 2021

Keywords:
Penultimate Glacial Cycle
Last Glacial Cycle
Deglaciation
^{36}Cl cosmogenic isotope
Serra da Estrela
Portugal

ABSTRACT

The objective of this work is to present a first assessment on the age of the glacial features of the Serra da Estrela, in the central Portugal, Iberian Peninsula (40°19′ N, 7°37′ W, 1993 m), using Cosmic-Ray Exposure dating (in situ cosmogenic ^{36}Cl). A total of 6 samples were dated, 4 extracted from exposed moraine boulders and 2 from glacially polished bedrock surfaces. Despite the low number of samples, the results are consistent, reinforcing previous dating obtained by other methods and geomorphological and paleoclimatic information. The maximum extension of the glaciers occurred at the end of the Penultimate Glacial Cycle (Marine Isotope Stage 6), during Heinrich Stadial 11, around 140 ka. At the end of the Last Glacial Cycle, slightly before the Last Glacial Maximum, at around 30 ka, the Estrela glaciers reached again a similar extent. Finally, the glaciers disappeared from the Serra da Estrela at the beginning of the Bølling-Allerød Interstadial, at around 14.2 ka. These data confirm a certain synchronicity in the major glacial phases in most the Mediterranean and also European mountains, although there are notable differences in the maximum extent in the two cycles.
© 2021 The Authors. Published by Elsevier B.V. This is an open access article under the CC BY-NC-ND license (http://creativecommons.org/licenses/by-nc-nd/4.0/).

1. Introduction

Recent research has contributed to significant advances on the understanding of the glacial chronology of the Iberian mountains, but it has focussed mainly in the end of the last glacial cycle and Holocene. However, the period when the glaciers reached their Maximum Ice Extent (MIE) in the Iberian Peninsula is still poorly known (Oliva et al., 2019).

The Maximum Ice Extent (MIE) was not contemporaneous with the Last Glacial Maximum (LGM) in all the mountain ranges of Iberia. According to Clark et al. (2009), the LGM occurred from 26.5 to 19 ka, when the sea reached its last lowest level, although in fact the concept of "global" for this period is in question in relation to glacial expansion (Hughes et al., 2013). In the Pyrenees, the MIE during Last Glacial Cycle (115–11.7 ka; LGC) occurred at 60 ka (García-Ruiz et al., 2003, 2010, 2013; Lewis et al., 2009; Delmas, 2015), while in the Cantabrian mountains (Rodríguez-Rodríguez et al., 2015, 2016), the northwest Iberian mountains (Rodríguez-Rodríguez et al., 2014), the Central System (Palacios et al., 2012a; Domínguez-Villar et al., 2013; Pedraza et al., 2013) and the Sierra Nevada (Gómez-Ortiz et al., 2012, 2015), it took place closer to the LGM at 35 to 31 ka.

The LGM is marked by an important and long glacial advance in all the mountains of the Iberian Peninsula and is responsible for the largest and best-preserved moraines (Delmas, 2015). Their ages have been mainly obtained by Cosmic-Ray Exposure (CRE) dating and show multiple small glacial advances and recession episodes between 26 and 21 ka. Large polygenetic moraines formed in narrow glacial valleys, while in unconstrained conditions, the glaciers gave origin to multiple moraine ridges (Palacios et al., 2015). This situation occurs in the Pyrenees (Delmas, 2015; Turu et al., 2016), in the Cantabrian and northwest Iberian mountains (Rodríguez-Rodríguez et al., 2014, 2015, 2016; Serrano et al., 2015, 2017), in the Central System (Palacios et al., 2012a and 2012b; Andrés and Palacios, 2014; Carrasco et al., 2015) and in the Sierra Nevada (Gómez-Ortiz et al., 2012, 2015; Oliva et al., 2014, Palacios et al., 2016).

Contrasting with the knowledge on the MIE during the LGC, the understanding of pre-LGC glacial events in the Iberian Peninsula remains poor. Glacial landforms older than LGC have been dated only in very few locations of the central Pyrenees, the central Cantabrian Mountains, mountain ranges of NW Iberia and Sierra Nevada. In the south of the central Pyrenees, Lewis et al. (2009) applied optically stimulated

* Corresponding author.
E-mail address: vieira@edu.ulisboa.pt (G. Vieira).

https://doi.org/10.1016/j.geomorph.2021.107781
0169-555X/© 2021 The Authors. Published by Elsevier B.V. This is an open access article under the CC BY-NC-ND license (http://creativecommons.org/licenses/by-nc-nd/4.0/).

luminescence (OSL) techniques to fluvioglacial terraces and on overlying aeolian silt, with results indicating glacial periods at 151 ± 11 ka in the Gállego valley, and at 178 ± 21 ka in the Cinca valley. Elsewhere in the Pyrenees, García-Ruiz et al. (2013) also applied OSL dating methods in the Aragón valley fluvioglacial terraces, with results showing two glacial phases at 171 ± 22 and 263 ± 21 ka. Moreover, Rodríguez-Rodríguez et al. (2016) applied CRE (^{10}Be) dating to erratic and moraine boulders in the Porma valley (central Cantabrian Mountains) and yielded ages of 134 ± 4 ka and 169 ± 6 ka. In adition, an age of 286 ± 6 ka from an erratic was considered an outlier. Villa et al. (2013) applied U/Th dating to the limestone of cemented calcareous breccias in Duje valley, in Picos de Europa, also in the central Cantabrian mountains. These breccias are resting on glacially abraded surfaces and are covered by moraines. The oldest dates obtained for the base of the breccias are between 276 ± 23 ka and 394 ± 50 ka. Vidal-Romaní and Fernández-Mosquera (2006), Vidal-Romaní et al. (2015) applied CRE (^{21}N) dating in two ranges of the NW of the Peninsula: in the Sierra de Queixa, a maximum advance was dated at 155 ± 30 ka, and in the Serra de Gerês/Xurez, polished bedrock outcrops were dated at 231 ± 48 ka and 131 ± 31 ka. Palacios et al. (2019) applied CRE (^{10}Be) dating to the most external moraine boulders in the Mulhacen valley (Sierra Nevada) and obtained ages of 134.8 ± 10 ka and 129.2 ± 8.9 ka.

The identification of pre-LGC glacial landforms is still lacking in the Iberian Range and in the Central System, although its existence has long been postulated (Lotze, 1962; Obermaier and Carandell-Pericay, 1917). However, after the application of modern dating methods, many of the landforms thought to be pre-LGC in most of the Iberian mountains turned out to result from pulses within the LGC (Oliva et al., 2019). The scarce evidence of MIE of pre-LGC ages in Iberia contrasts with the data from other Mediterranean mountains, such as the Apennines (Kotarba et al., 2001; Giraudi et al., 2011; Giraudi and Giaccio, 2017) and the Balkans (Hughes et al., 2006a, 2006b, 2007, 2010, 2011; Žebre and Stepišnik, 2014, 2015; Adamson et al., 2017; Leontaritis et al., 2020).

The Serra da Estrela, the highest mountain of the western and moister sector of the Central System, shows extremely well-preserved glacial landforms and deposits, but with a still very poorly constrained chronology (Fig. 1). The glacial geomorphology of the area was studied in detail by Lautensach (1929; 1932), Daveau (1971) and Vieira (2004). Daveau (1971) suggested the possibility for a pre-LGC glaciation following the identification of sparse boulders in the Lagoa Seca site, which contrasted with other moraine deposist of the mountain. Based on geomorphological analysis, Vieira (2004) identified four general stages in the Estrela glaciation, including one probably pre-LGC with evidence in several areas in the plateaus. Using preliminary thermoluminescence (TL) dating from fluvioglacial sediments, he placed the MIE in the LGC at ca. 33 to 30 ka, a value in agreement with other Iberian mountains, but no further ages existed up to the present work on pre-LGC or LGC evidence.

The objective of this work is to present a first assessment on the age of the glacial features in Serra da Estrela using CRE methods (^{36}Cl). Aiming at identifying the age of the MIE during the LGC, or earlier, glacial boulders and polished surfaces, have been selected from key sites identified in previous studies. Vieira (2004, 2008) mentions the significance of the Estrela plateau for paleoenvironmental reconstruction based on its flat top morphology and elevation just above the

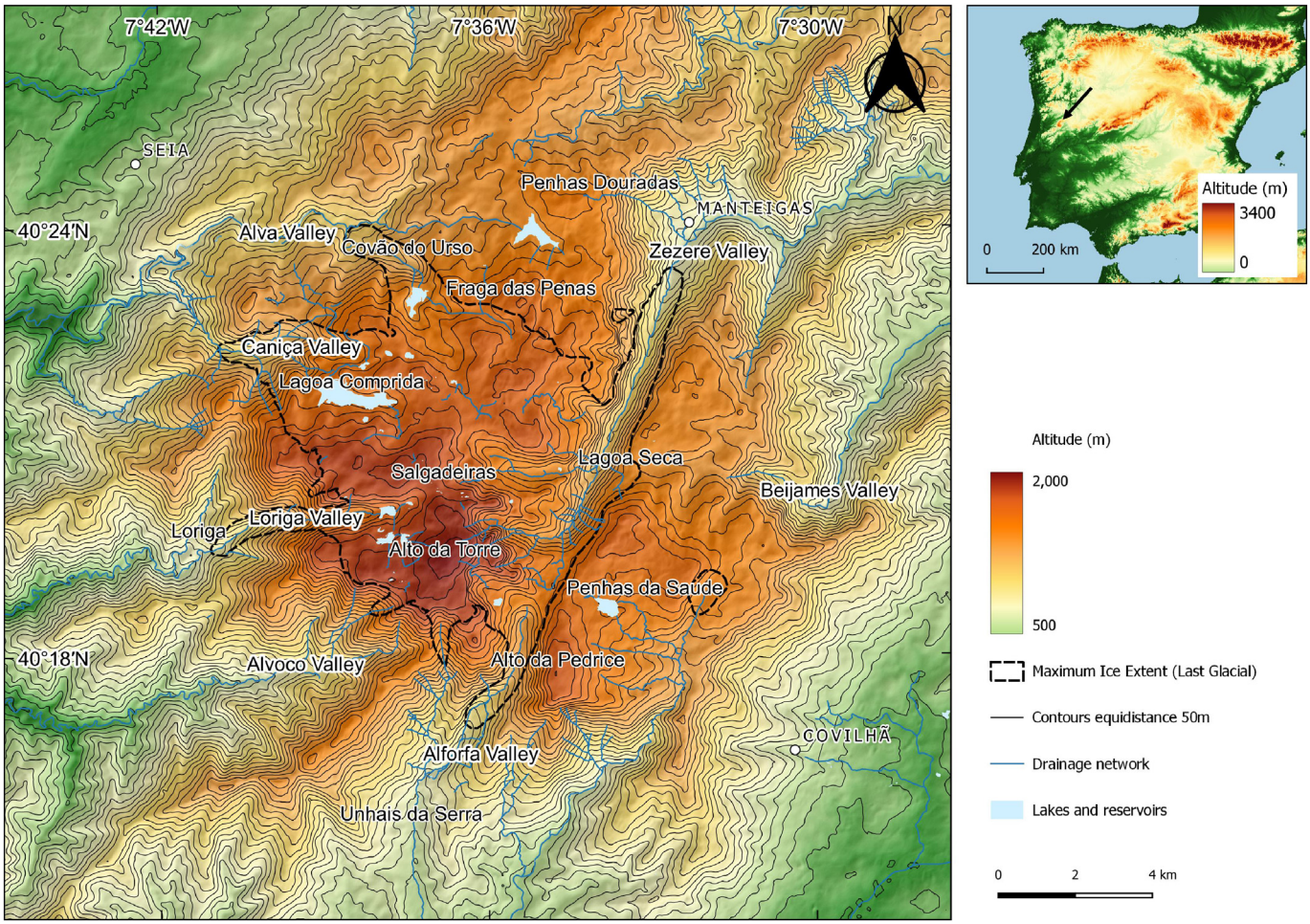

Fig. 1. Location and general characteristics of the Serra da Estrela. The Maximum Ice Extent is derived from Vieira (2004).

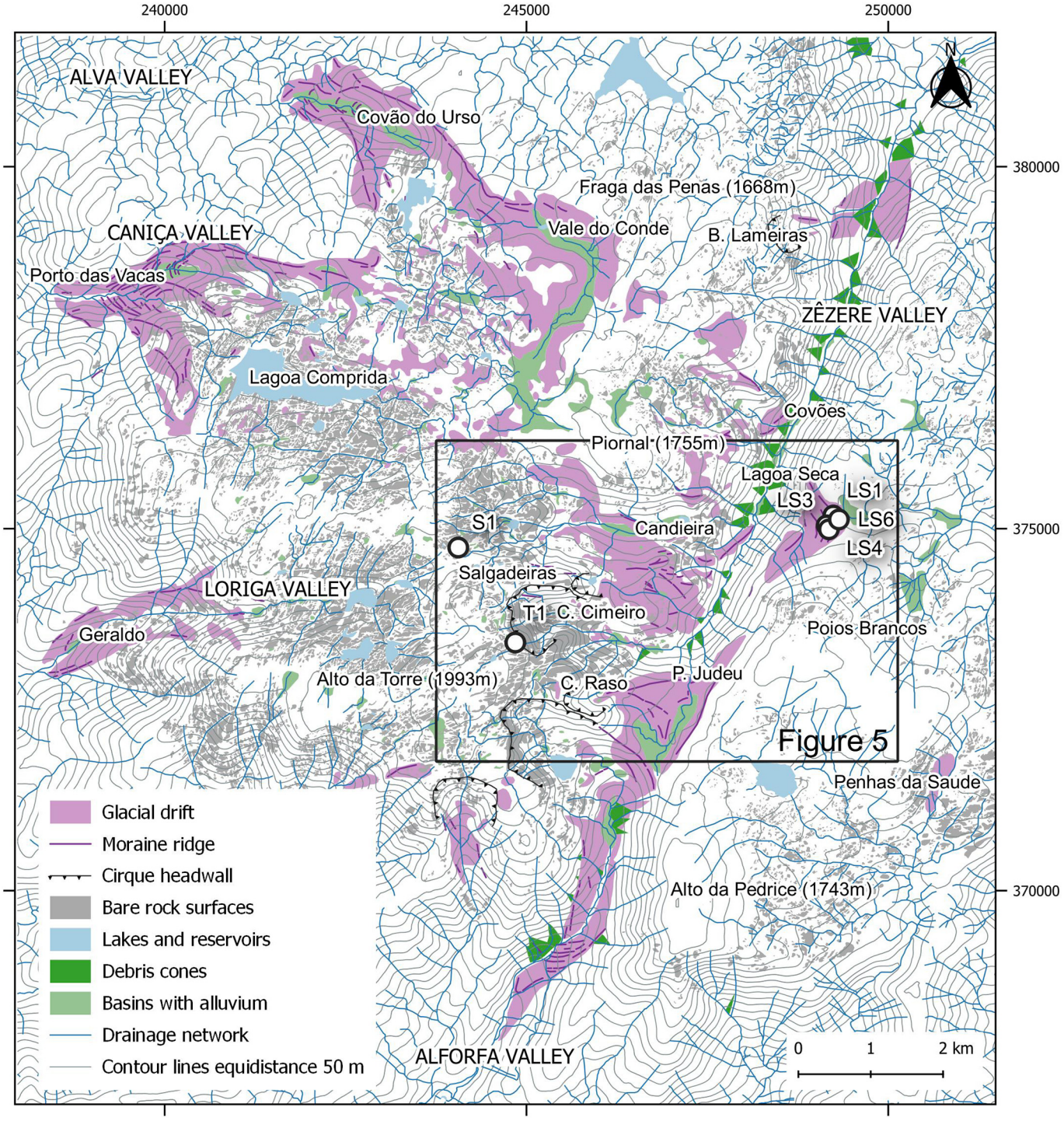

Fig. 2. Distribution of moraines and glacial erosion features in the Serra da Estrela and location of Fig. 5. The map is based in Vieira (2004).

equilibrium line altitude (ELA) at the MIE. This would have generated glaciers with high climatic sensitivity, reacting fast and extensively to even small changes in the ELA. Hence, the Estrela may bear important evidence to bridge the gap between the Sierra Nevada, in the Southeast, and the mountains of Northwest and North of Iberia and to identify remnants of an older glacial event in the Central System.

2. Study Area

The Serra da Estrela is a granite plateau mountain in Central Portugal rising to 1993 m a.s.l. at Alto da Torre (40°19′ N, 7°37′ W), making it the highest elevation in mainland Portugal (Fig. 1). Estrela is part of the Central System and is limited by two steep fault scarps with a general SW-NE direction and with a relative relief of over 1200 m. The upper area has two plateaus, divided by the NNE–SSW tectonic lineament of the Zêzere and Alforfa valleys. The western plateau is the highest at 1400–1993 m while on the eastern plateau altitudes stay below 1750 m. The mountain forms a major condensation barrier to the moist air masses from the Atlantic, entering the Iberian Peninsula from the west. In the present-day, annual precipitation reaches ~2500 mm, mean annual air temperatures are close to 4 °C at the summit and the climate is Mediterranean, with warm and dry summers (Mora, 2010).

Cabral (1884) showed for the first time the occurrence of glaciogenic features in the Estrela, but it was only with Lautensach (1929) that the glaciation was studied in more detail. He identified the presence of a large plateau ice-field with several radiating valley glaciers, described several moraines and presented an estimation of the glacier topography. Daveau (1971) revised Lautensach's ideas and presented a more comprehensive account of the glacial geomorphology of the mountain, improving mapping and the description of moraines and kame deposits. Vieira (2004) made a thorough study on the glacial geomorphology of the Estrela, including geomorphological mapping, sedimentological analysis of glacial and fluvioglacial deposits and modelling of the glacier surfaces (Fig. 2).

The glaciated area during the MIE was c. 66 km^2 and is well-defined by latero-frontal moraines in the valleys and ice-marginal moraine complexes (Vieira, 2004, 2008; Santos et al., 2020) (Fig. 2). Most of the glaciation occurred in the western plateau, between Alto da Torre and Fraga das Penas, where a plateau icefield with five main radiating valley glaciers (Zêzere, Alforfa, Loriga, Covão Grande and Covão do Urso) were present. On the eastern plateau, only small glaciers occurred, and geomorphological evidence of a widespread glaciation is lacking. Vieira (2008) reconstructed the plateau ice-field and valley glaciers based on the maximum extent of the clear glacial evidence and on physical-based modelling of glacier profiles. Fig. 3 shows the reconstructed glaciers as viewed from the north, with the east-west asymmetry in the plateaus and the main drainage along the Zêzere valley. The author identified a regional equilibrium line altitude (ELA) at c. 1650 m asl, with a west-east asymmetry in local ELA's associated to snow drift (lower ELAs in east-facing glaciers). A weak N-S asymmetry probably controlled by insolation differences was also found. The glaciers draining from the ice-field showing lowest ELAs were those facing NE and SSE (1570–1590 m), while those facing S and SW showed the highest ELAs (>1700 m). A key result of that study was the analysis of the glacier hypsometric curves, which revealed a high climatic sensitivity of the Estrela glaciers, as typical of plateau ice-fields with a large area above the ELA.

The western plateau, especially above 1650 m, shows extensive granite outcrops without significant moraine deposits, but with extensive glacial scouring, knock-and-lochan morphology and roches moutonnées (Fig. 4). Sectors with widely spaced joints (tens of meters) gave origin to massive and glacially polished flat rock surfaces (e.g. Lagoa do Peixão area), while more closely spaced joints favour the development of roches moutonnées (e.g. upper valley of Loriga). Post-glacial weathering has lowered most of the granite surfaces a few centimetres, especially in the coarse-grained variants, as shown by glacially polished quartz veins standing out above the surrounding granite surfaces showing a post-glacial lowering of 1–3 cm (Vieira, 2004). At some sites fresh polished surfaces show striations and shatter marks. The best polished outcrops occur in medium to fine-grained granite variants, both near the plateau margins, where glacial erosion was more intense, or in knobs in the glacial cirques or upper overdeepenings along the valleys (Migoń and Vieira, 2014). Key sites occur at Salgadeiras, Alto da Torre, Lagoa Comprida and Covão Cimeiro (Figs. 2 and 4).

Tors and the weathering mantle are lacking in the highest areas and only occur in small patches where glacial erosion was limited or where tor exhumation is post-glacial (Ferreira and Vieira, 1999; Vieira and Nieuwendam, 2020). Cirques are present mainly in the eastern side of the plateau and the areas where glacial erosion was strongest still show widespread bare rock outcrops. In the western plateau, the northern areas between 1500 and 1600 m lack traces of glacial erosion, moraines and, in some areas, show remnants of weathering mantle. The valleys show typical geomorphological features of the glaciated valley landsystem, with cirques, u-shaped cross-sections, overdeepenings (above ~1200 m a.s.l.), moraines and kame terraces (Fig. 5). The largest moraine accumulations are mainly located in the five radial valleys with some also occurring in the plateau (e.g. Vale do Conde moraine complex) and allowed for identifying four general stages in the Estrela glaciation (Vieira, 2004):

(i) The external stage marks the outer limits of the glacial deposits and is shown by the peripheral moraines outside of the main and best preserved moraine in Lagoa Seca and by a small probable till outcrop ca. 600 m downstream, by the large boulders of possible glacial origin at Barroca das Lameiras, the Penhas da Saúde till and boulders at Cântaro Raso. These deposits occur between a few hundred metres and c. 2 km from the main moraines, except the case of the Penhas da Saúde till, which occurs

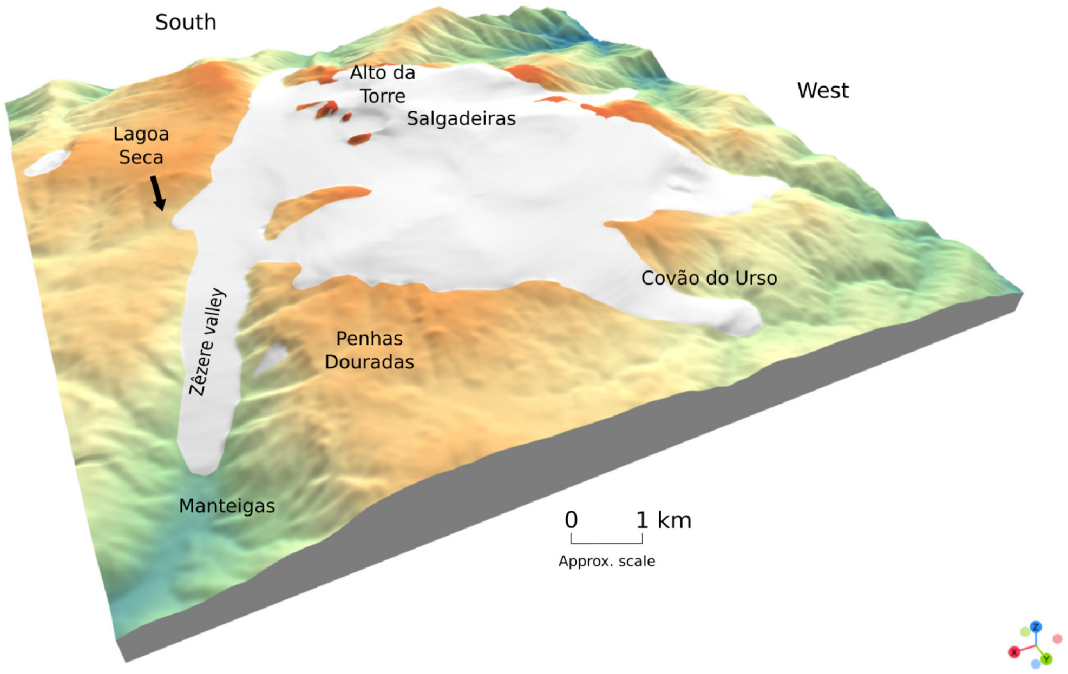

Fig. 3. Reconstruction of the Serra da Estrela Plateau ice-field and valley glaciers based on the maximum ice extent as identified by geomorphological evidence (see Vieira, 2008).

Fig. 4. Glacial erosion landscape in the Lagoa Comprida area.

in the eastern plateau, where unequivocal glacial landforms are lacking. The external moraines at Lagoa Seca and Barroca das Lameiras are poorly preserved and the matrix is lacking.

(ii) The main latero-frontal moraines stage is present in all the valleys and is marked by well-developed moraine ridges. These are generally composed of a coarse sandy-gravelly diamicton with large sub-rounded c. 1–5 m granite boulders, which are prominent in the surface due to the erosion of the matrix. In some valleys, this stage is composed of 2 to 4 moraine ridges (Covão do Urso, Loriga, Porto das Vacas and Lagoa Seca). This stage was preliminarily dated applying thermoluminescence to massive fluvioglacial silts from an intermoraine depression at Lagoa Seca and to a fluvioglacial deposit from a terrace at the Alva Valley, having provided ages of 30 ± 4.5 TL ka and 33.1 ± 5.0 TL ka BP respectively (Vieira, 2004). These results suggest that this stage occurred slightly before the LGM.

(iii) The Internal Stages 1 and 2 are characterized by the presence of moraine ridges confined to the valleys already in recession compared to the previous stage. The presence of a large number of moraine ridges within a few hundred meters in several valleys

Fig. 5. The upper sector of the Zêzere valley with the lateral moraine of Poio do Judeu on the left site and the cirque of Covão Cimeiro in the background.

(12 in Alva, 8 in Caniça and 9 in Alforfa valleys) marks the Internal Stage 1, which seemingly was characterized in different valleys by several episodes of retreat and readvance. The moraines of Poio do Judeu, Covões and Geraldo have been included in this stage, because they show a first stabilization after an initial retreat. The Internal Stage 2 shows various stabilization stages after a very significant glacier retreat and includes smaller moraines. Palynological analysis and radiocarbon ages from organic infills of the Candieira Lake at 1320 m a.s.l. suggest that the valley was deglaciated at 14.8 cal ka BP but the glaciers were still present in the higher parts of the catchments (Van der Knaap and Van Leeuwen, 1997).

3. Methods

3.1. Geomorphological mapping

Field surveying and geomorphological mapping was the basis to identify the different glacial stages, with the main interpretation deriving from the geomorphological map by Vieira (2004) with minor corrections from the analysis of recent Google satellite imagery in QGIS 3.16. The original map was produced based on extensive field surveys at 1:10000 scale, aerial photo interpretation and high resolution orthophotomap analysis.

The Lagoa Seca moraine, which is our main sampling site, was surveyed in August 2019 using an unmanned aerial vehicle (UAV; DJI Phantom 3 advanced). The flight was conducted at 80 m above the ground, with a 12.4MP camera, which allowed for the production of an orthomosaic and a digital surface model with a spatial resolution of 3.5 cm. Processing was done using PIX4D mapper. From the latter, a hillshade model and contour elevation map were produced, and were the basis for the detailed geomorphological mapping of the Lagoa Seca site.

3.2. Selection of CRE sample sites

The geomorphological analysis guided the selection of the sampling locations. The objective was to select the best sites to constrain the age of the phases of the glaciation of the Serra da Estrela: (i) the MIE, (ii) the major moraines phase and (iii) the deglaciation (Fig. 5). In this study, we did not aim at dating the moraines present along the valleys and described by Vieira (2004) as internal stages 1 and 2.

The Lagoa Seca col. (Figs. 5, 6 and 7) was selected for dating the MIE (i) and the major moraines phase (ii), thanks to the presence of several moraine ridges with different degrees of degradation. The site is a wide col. at c. 1300 m altitude at the eastern interfluve bounding the Zêzere valley, where the longest glacier of the Estrela flowed for c. 11 km (Fig. 3). At that site, the Zêzere glacier showed a small transfluence into the adjacent Beijames valley headwaters, having deposited at least five moraine ridges (Soncco, 2020) formed by very large boulders (> 2 m), showing that the upper Zêzere valley was fully glacier ice infilled (Daveau, 1971; Vieira, 2004, 2008).

The external moraines of Lagoa Seca col. (ridge 1 and 2) define the MIE in Serra da Estrela (Figs. 7 and 8). These moraines are very degraded boulder lineaments and do not form evident ridges nowadays, and they lacking the coarse sandy-gravelly moraine body that occurs in the

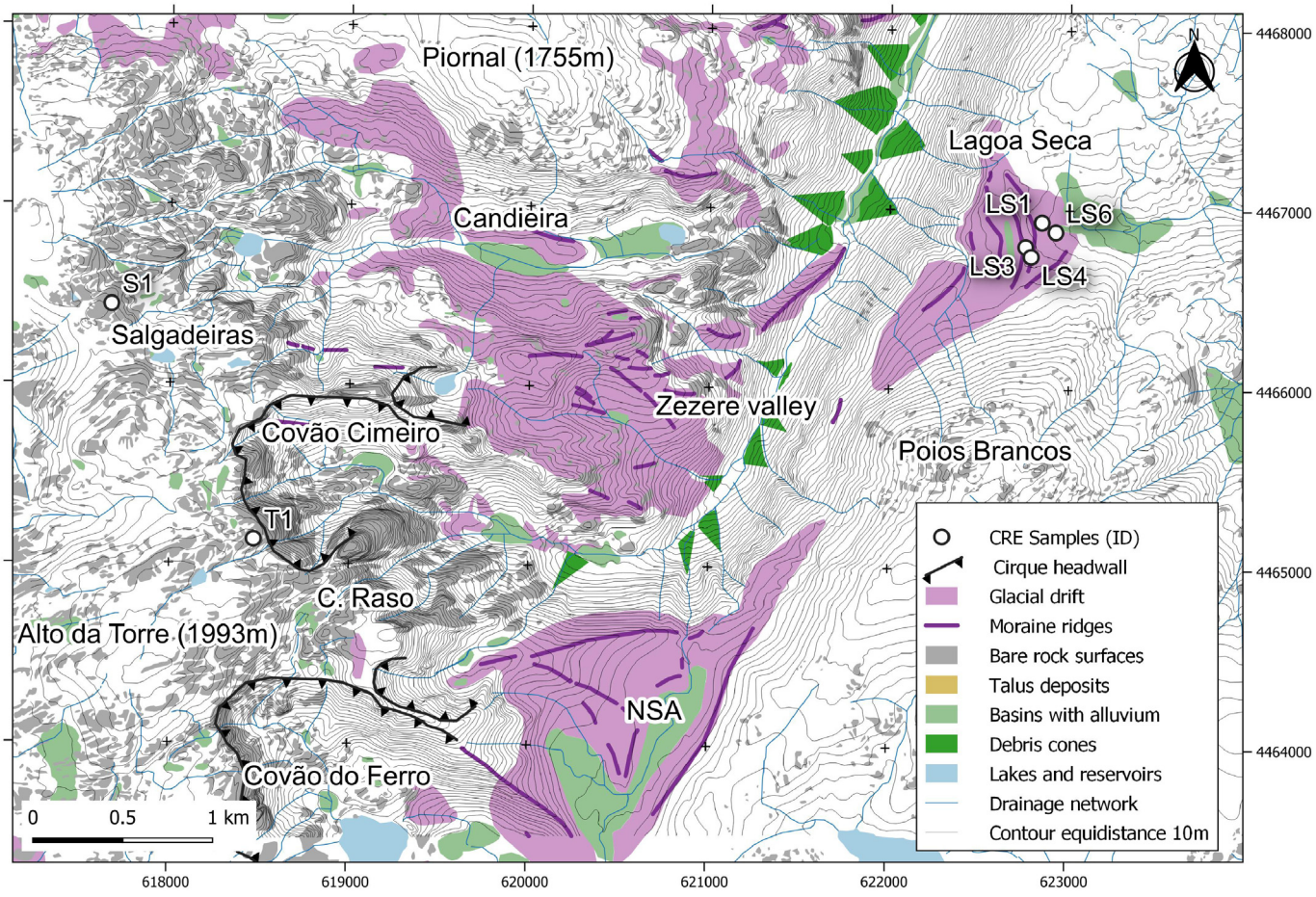

Fig. 6. Geomorphological map of the upper Zêzere valley and Torre Plateau with the location of the sampling sites.

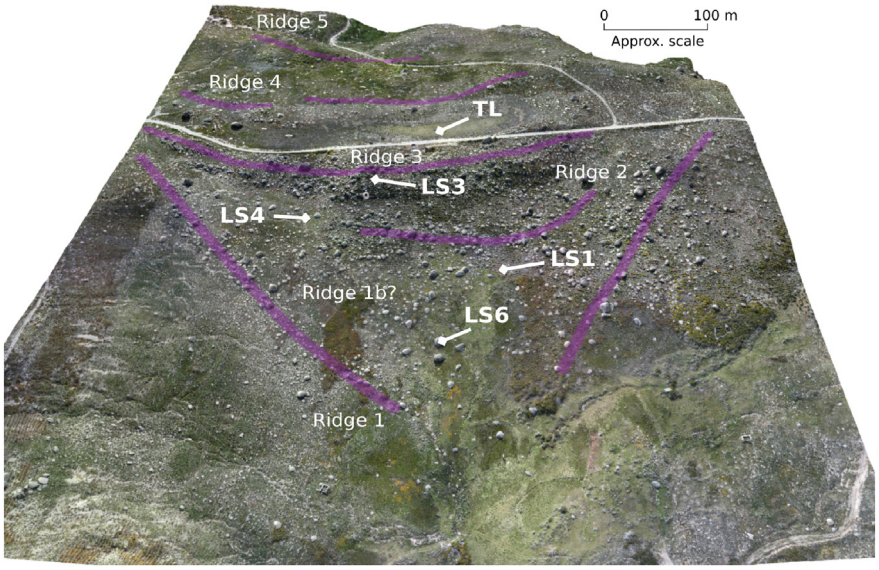

Fig. 7. 3D model of the Lagoa Seca with a view towards the Zêzere valley (westwards). This model results from a UAV survey conducted in 2017 that covers a larger area than the one of 2019 used for the mapping.

internal ones. In the external moraines, several large boulders show weathering pits that are larger and deeper than the ones in the internal moraines. The position of the boulders, their linear distribution and symmetry in both sides of the valley, as well the distance to the Poios Brancos slope and lack of geomorphic evidence of an in situ position, support their glacial origin. These features are very different from

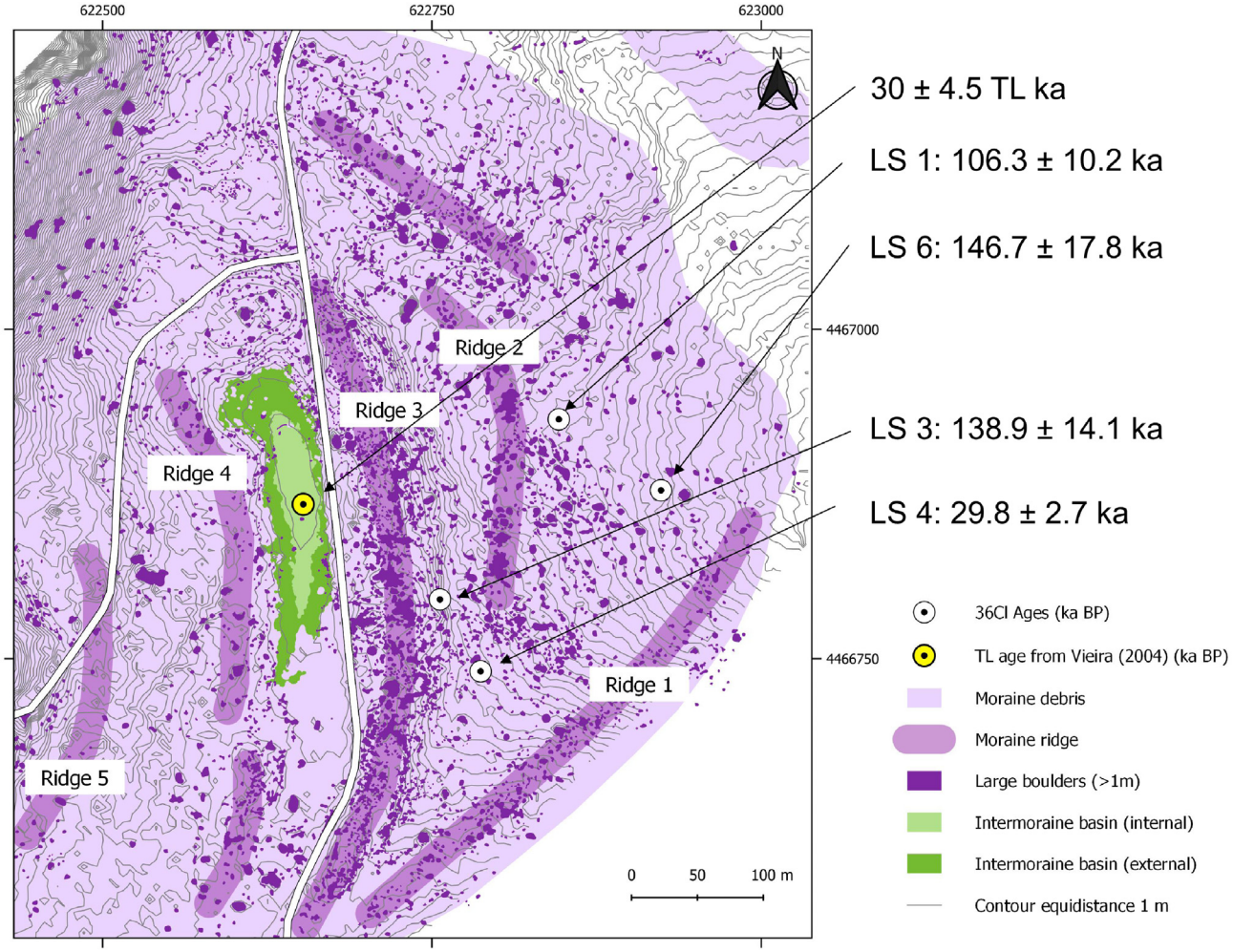

Fig. 8. Lagoa Seca col. with location of the dated boulders, as well as the TL dated fluvioglacial sediment by Vieira (2004).

other sites of the Estrela, where boulders are clearly exhumated saprolites (see e.g. Migoń and Vieira, 2014).

Three samples were collected from the external moraines (Fig. 9): sample LS6 was collected in the more external ridge (ridge 1) and two samples were collected in the second peripheral moraine (ridge 2 - LS1 and LS4).

The more internal zone of ridge 2 was overridden by a large and much better-preserved moraine from the major moraines phase (ii). This moraine (ridge 3) closes the intermoraine basin of Lagoa Seca, which is filled with fluvioglacial deposits, previously dated by thermoluminescence at provided an age of 30 ± 4.5 ka (Vieira, 2004). Sample LS3 was collected from the moraine ridge 3 aiming at dating the major moraines phase (Figs. 7, 8 and 10).

For the last phases of deglaciation, bare granite polished surfaces were selected. One sample (T1) was collected on the summit surface of Serra da Estrela, in the Torre plateau just above the headwalls of the Covão Cimeiro Cirque at 1934 m. With this sample we wanted to determine the age of the melting of the Estrela plateau ice field. The other bedrock sample (S1) was collected from a glacial polished surface at Salgadeiras at 1851 m, on the first step below the Torre plateau. The wall of this step faces NE, the most suitable for glacier maintenance due to the shady and leeward setting. With this sample we wanted to determine the age of the last deglaciation at a site where the glacier would have melted the latest (Fig. 11).

3.3. Cosmogenic-ray exposure dating

A total of 6 granite samples with thicknesses of 2–5 cm were extracted using hammer and chisel, 2 from bedrock polished surfaces and 4 from the surficial layer of moraine boulders >1 m-high standing on stable, gently sloping surfaces (Table 1). Stable and well-embedded boulders far from the influence of slope processes were preferred so that the potential risk of overturning is minimized. Aiming to ensure the optimal exposure to the cosmic-rays, flat and gentle rock faces were preferred to sharp crests and steep sides. To minimize previous burial or snow cover interference, large boulders were selected. Horizon shielding was measured at each sampling site using a compass and clinometer at 10° azimuth intervals.

We selected the ^{36}Cl cosmogenic nuclide for CRE dating method, as it has been previously used successfully in other sites on the Central System (Palacios et al., 2011, 2012a, 2012b). Previous studies have used the ^{10}Be isotope, also successfully (Domínguez-Villar et al., 2013; Carrasco et al., 2015), but Palacios et al. (2017a) and Andrés et al. (2018) demonstrated that the results obtained with both isotopes are fully comparable.

We followed the laboratory procedures for ^{36}Cl analysis in whole rock (Zreda et al., 1999; Phillips, 2003). Whole rock samples were crushed and pulverized using a roller grinder. The samples were then sieved to separate the sand size fraction and leached in deionized water and HNO_3 to remove atmospheric Cl. Next, they were dissolved in a hot mixture of hydrofluoric and nitric acids, and $AgNO_3$ was added to the solution to precipitate AgCl. Sulphur was separated by precipitating $BaSO_4$. A spike of isotopically enriched ^{35}Cl was added during the dissolution process. This isotope dilution mass spectrometry method enabled the sample Cl content to be determined from accelerator mass spectrometry (AMS) analysis (Ivy-Ochs et al., 2004; Desilets et al., 2006). The AMS analysis of the ^{36}Cl/Cl and ^{37}Cl/^{35}Cl ratios in the AgCl targets was carried out at the PRIME Laboratory (Purdue University, USA). The ^{36}Cl data is presented in Table 1.

Aliquots of rock, pre-treated (bulk rock) and post-treated (target fraction), were powdered and analyzed for: (i) Major elements, using fusion inductively coupled plasma optical emission spectrometry (ICP-OES), (ii) Trace elements, using inductively coupled plasma mass spectrometry (ICP-MS); and (iii) Boron, using prompt-gamma neutron

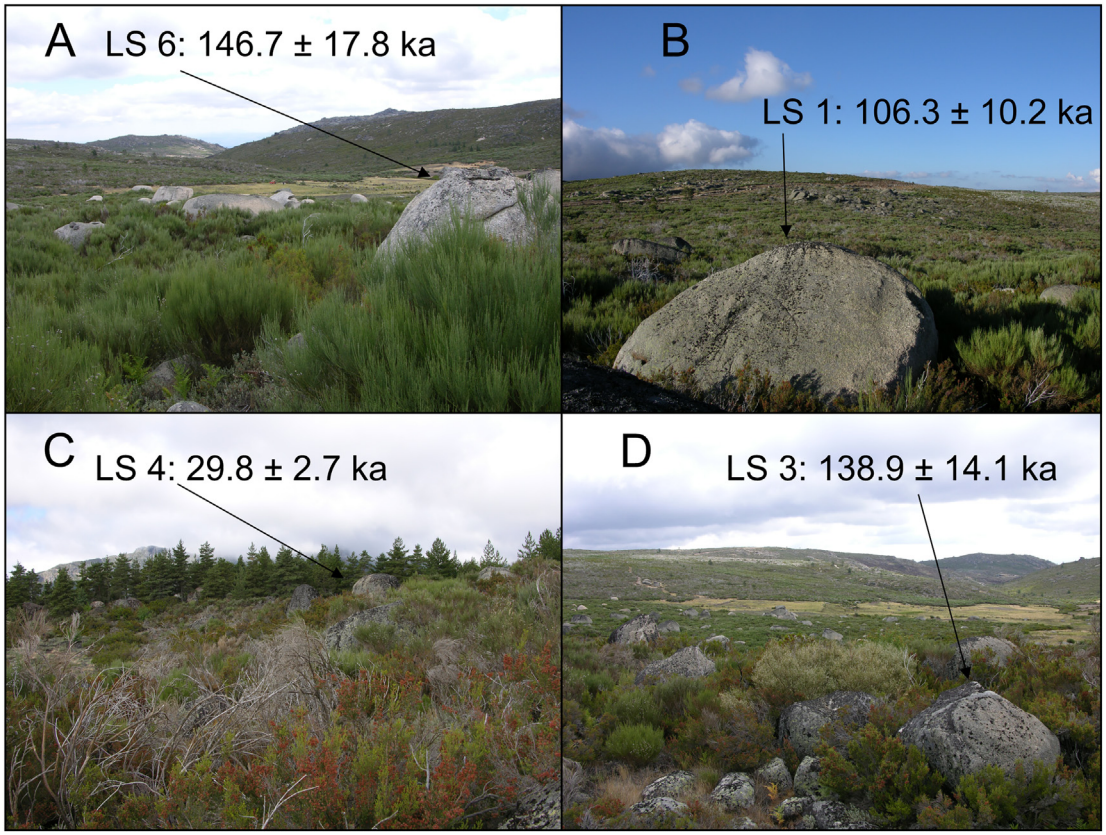

Fig. 9. Location of the sampled moraine boulders at the Lagoa Seca col. A) Sample LS6; B) Sample LS1; C) Sample LS4; D) Sample LS3.

Fig. 10. The Lagoa Seca moraine with the ridge 4 (left) and ridge 3 (right) and the small intermoraine basin.

activation analysis (PGNAA) at the Activation Laboratories (Ancaster, Canada). The element concentrations of bulk rock were obtained from two samples and the average was used, as the lithology of all samples was very similar (Table 2). The element concentrations of the target fractions are exposed in Table 3.

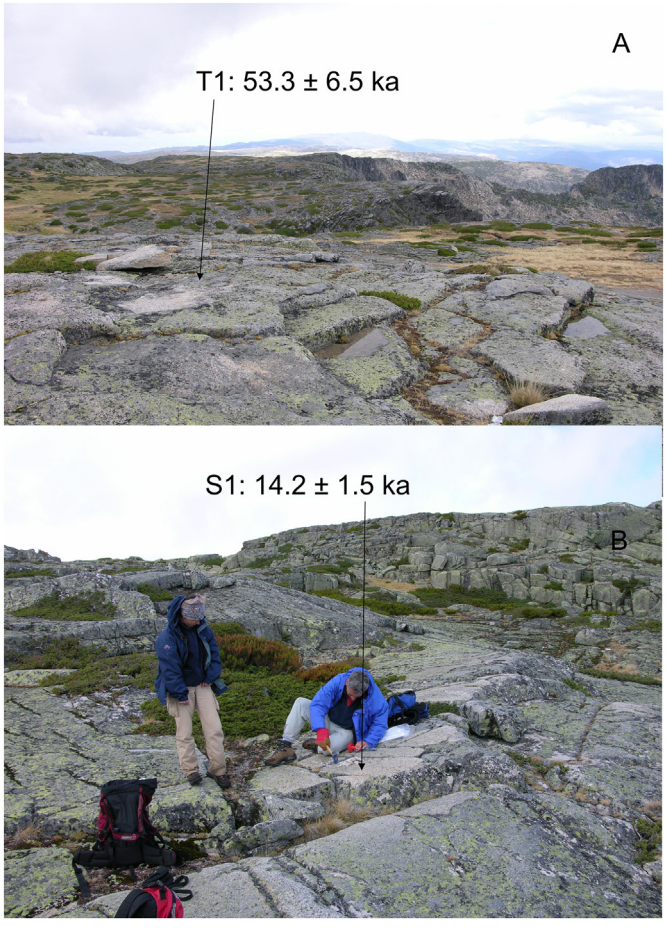

Fig. 11. Sampling sites of bare rock surfaces at the western plateau: A) the Torre plateau (T1) site above the Covão Cimeiro cirque B) the Salgadeiras polished rock surface (S1).

The exposure ages were calculated using the spreadsheet for in-situ ^{36}Cl exposure age calculations by Schimmelpfennig (2009) and Schimmelpfennig et al. (2009). We used the cosmogenic ^{36}Cl production rates for Ca spallation by Stone et al. (1996) (48.8 ± 3.4 atoms ^{36}Cl (g Ca)$^{-1}$ a^{-1}); for K spallation by Schimmelpfennig et al. (2014) (148.1 ± 7.8 atoms ^{36}Cl (g K)$^{-1}$ a^{-1}); for Ti spallation by Fink et al. (2000) (13 ± 3 atoms ^{36}Cl (g Ti)-1 a-1); and for Fe spallation by Stone et al. (2005) (1.9 atoms ^{36}Cl (g Fe)-1 a-1). The production rate used for epithermal neutrons for fast neutron in the atmosphere at the land/atmosphere interface was 696 ± 185 neutrons (g air)$^{-1}$ yr^{-1} (Marrero et al., 2016). The high energy neutron attenuation length applied was 160 g.cm^{-2}.

The in situ accumulation of ^{36}Cl depends on various factors including latitude, elevation, sample thickness, surrounding topography and snow cover. The elevation–latitude scaling factors for nucleonic and muonic production were evaluated using CosmoCalc (Vermeesch, 2007), based on the scaling model by Stone (2000). The shielding factor has been calculated using the Topographic Shielding Calculator v1.0 of CRONUS-Earth Project (2020). We also used CRONUS-EARTH ^{36}Cl to calculate the exposure ages. A 0 erosion rate has been considered in the calculation of the ages, since it was not possible to determine in the field the erosion suffered by the sampled surface. In any case, an attempt was made to sample the surface that appeared to be closest to the original glacial surface. We used the results from the spreadsheet by Schimmelpfennig et al. (2009) in the analysis (Table 4). They are very similar to those from the CRONUS-Earth Project calculator, with differences of less than 5%.

4. Results and discussion

4.1. Cosmogenic-ray exposure ages

The CRE results obtained in the Lagoa Seca col. (Table 4) confirm the previous geomorphological observations and the chronological differentiation between the peripheral moraines and the main moraine (Figs. 6, 7 and 8). The samples collected in the peripheral moraines (i), which, according to geomorphological observations, have been attributed to the MIE in Serra da Estrela, yielded the ages of 146.7 ± 17.8 ka (LS6), 106.3 ± 10.2 ka (LS1) and 138.9 ± 14.1 ka (LS3), with an

Table 1
Geographic sample locations, topographic shielding factor, sample thickness and distance from terminus.

Sample name	Type	Latitude (°N)	Longitude (°W)	Elevation (m a.s.l.)	Shielding factor	Thickness (cm)
LS 1	Moraine boulder	40.3439	7.5534	1421	0.9924	1.3
LS 3	Moraine boulder	40.3427	7.5546	1425	0.9693	2.0
LS 4	Moraine boulder	40.3421	7.5541	1426	0.9993	3.0
LS 6	Moraine boulder	40.3435	7.5526	1411	0.9702	5.0
T1	Glacial polished bedrock surface	40.3265	7.6045	1934	0.9995	2.0
S1	Glacial polished bedrock surface	40.3383	7.6137	1851	0.9984	3.0

Table 2
Chemical composition of the bulk rock samples before chemical treatment. The figures in italics correspond to the average values of the bulk samples analysed and were those used for the age-exposure calculations of those samples without bulk chemical composition analysis.

Sample name	CaO (%)	K_2O (%)	TiO_2 (%)	Fe_2O_3 (%)	Cl (ppm)	SiO_2 (%)	Na_2O (%)	MgO (%)	Al_2O_3 (%)	MnO (%)	P_2O_5 (%)	CO_2 (%)	B (ppm)	Sm (ppm)	Gd (ppm)	Th (ppm)	U (ppm)
LS 4	0.430	5.450	0.131	1.430	23	73.610	3.110	0.150	14.570	0.031	0.430	–	12.1	18	1.3	5.0	8.3
S1	0.330	3.960	0.035	1.050	16	72.660	4.040	0.050	15.020	0.046	0.430	–	15.9	0.5	0.4	1.6	10.4
Average	*0.380*	*4.705*	*0.083*	*1.240*	*19.5*	*73.135*	*3.575*	*0.100*	*14.795*	*0.0385*	*0.430*	–	*14*	*9.25*	*0.85*	*3.3*	*9.53*

arithmetic mean of 130.6 ± 14.0 ka ($n = 3$). The sample taken from the main moraine (ii), which overrides the western sector of the previous ones, yielded an age of 29.8 ± 2.7 ka (LS4).

A sample T1, from the Torre plateau at 1934 m yielded an age of 53.3 ± 6.5 ka and the sample S1 located bellow the Torre plateau, at the plateau margin in the headwaters of the Candieira valley, at 1851 m, yielded an age of 14.2 ± 1.5 ka (Fig. 11).

4.2. Analysis and geomorphological consistency of the CRE results

Geomorphological observations allowed to identify the position of the MIE of Serra da Estrela, which corresponds to the outermost moraines (i), showing highest weathering on the surface of the boulders and scarce or absent matrix. The CRE ages, with an average of 130.6 ± 14.0 ka (n = 3), place these moraines close to the Penultimate Glacial Cycle (PGC), centred at ~140 ka Marine Isotope Stage (MIS) 6 (Rohling et al., 2017), in particular during Heinrich Stadial 11 (HS-11) which took place at the transition from MIS 6 and interglacial or MIS 5e (Oppo et al., 2006). Previous studies show that the high intensity of weathering in moraines from the PGC may result in an underestimation of CRE ages (Briner et al., 2005; Schaefer et al., 2008; Balco, 2011). For this reason, it is recommended to use the age of the oldest boulder for the age of the moraine (Balco, 2011). If we follow this advice, the age the peripheral moraines would be 146.7 ± 17.8 ka for the outermost ridge (sample LS6, ridge 1) and 138.9 ± 14.1 ka for the innermost ridge (sample LS3, ridge 2).

We have only one sample for the main moraine of stage (ii) in the ridge 3, at Lagoa Seca col. (sample LS4), which limits the interpretation. However, its age of 29.8 ± 2.7 ka agrees with its better preservation, as shown by the presence of a sandy-gravelly matrix, as well as by the less weathered boulder surfaces. But above all, it shows a similar age to that of the 30 ± 4.5 TL ka fluvioglacial sediments (Vieira, 2004) that are enclosed by the moraine ridge 3. This clearly frames the formation of the moraine within the maximum expansion of the LGC.

Fig. 12 synthesises the reconstruction of the glacial evolution of the Lagoa Seca site: the oldest deposits are from the MIS 6 with LS6 at 146.7 ± 17.8 ka. LS3 with a slightly younger age and retreat position close to ridge 2, has deposited later at 138.9 ± 14.1 ka. During the Eemian, subaerial erosion prevailed, leading to the possible exhumation of LS1 at 106.3 ± 10.2 ka. The next glacial that is present at Lagoa Seca occurred at 29.8 ± 2.7 ka, which resulted in the built up of the large moraine ridge 3 and pushed forward LS3 that had been deposited previously. This age agrees with the existing ages of the fluvioglacial deposits in the intermoraine basin, showing that the glacier retreated to ridge 4 within that interval.

Sample S1, from glacial polish at the edge of the plateau at 1851 m in Salgadeiras, an area with favourable orientation for the preservation of glaciers due to its altitude and orientation, yielded an age of 14.2 ± 1.5 ka. This is in agreement with a radiocarbon age reported for the beginning of organic sedimentation in the Candieira lake (14.8 cal ka BP) some 3.2 km downstream in the same valley (Van der Knaap and Van Leeuwen, 1997). Both the ^{36}Cl and the ^{14}C ages suggest that the final deglaciation of the Serra da Estrela took place at the Bølling-Allerød Interstadial (B-A; 14.6–12.9 ka). The ^{36}Cl exposure age seems to exclude the formation of glaciers in the Serra da Estrela during subsequent cold periods such as the Younger Dryas, similarly to other Iberian mountains with limited altitude (García-Ruiz et al., 2016).

The only result which seems to be an outlier is T1, glacially abraded bedrock from the Torre plateau at 1934 m, with an age of 53.3 ± 6.5 ka, hence, much older than S1, which is in a lower position. This could mean that the plateau has not been covered by glaciers since that age, which is unlikely. If we consider that the sample was taken from a summit flat surface, where glacial erosion is minimal, even under a thick glacier, the age most likely denotes inheritance of cosmogenic ^{36}Cl from a previous phase of exposure. These situations are very common in samples located in such topographic situations and have been reported by several authors (e.g. Paterson, 1994; Briner et al., 2006; Bentley et al., 2006; Ivy-Ochs and Schaller, 2009; Balco et al., 2016).

Table 3
Concentrations of the ^{36}Cl target elements Ca, K, Ti and Fe, determined in splits taken after the chemical pre-treatment (acid etching).

Sample name	CaO (%)	K_2O (%)	TiO_2 (%)	Fe_2O_3 (%)
LS 1	0.17 ± 0.04	4.24 ± 0.42	0.07 ± 0.02	0.90 ± 0.18
LS 3	0.15 ± 0.04	4.42 ± 0.44	0.13 ± 0.03	1.38 ± 0.21
LS 4	0.11 ± 0.03	5.46 ± 0.27	0.11 ± 0.02	1.22 ± 0.18
L S 6	0.27 ± 0.07	4.11 ± 0.41	0.18 ± 0.04	1.61 ± 0.24
T1	0.06 ± 0.02	3.86 ± 0.39	0.09 ± 0.02	1.18 ± 0.18
S1	0.04 ± 0.01	3.75 ± 0.38	0.03 ± 0.01	0.95 ± 0.14

4.3. The results in the context of the Iberian Peninsula

In the study of the glacial chronology of the Iberian Peninsula, there was an initial exploratory period, when the different frontal moraine ridges of several glacial valleys were associated with the different glacial cycles proposed in the Alps (Oliva et al., 2019), mainly following the classical publications of Penck (1883) and Penck and Brückner (1909).

Table 4
^{36}Cl exposure ages from Serra da Estrela and related analytical data $^{36}Cl/^{35}Cl$ and $^{35}Cl/^{37}Cl$ ratios by PRIME Lab, Purdue University. See text for details on the calculation of exposure ages. The numbers in italics correspond to the internal (analytical) uncertainty at one standard level.

Sample name	Sample weight (g)	Mass of Cl in spike (mg)	$^{35}Cl/^{37}Cl$	$^{36}Cl/^{35}Cl$ (10^{-14})	[Cl] in sample (ppm)	[^{36}Cl] (10^4 atoms g^{-1})	Age (ka)
LS1	30.92	1.00	8.482 ± 0.066	175.578 ± 5.199	17.0	168.046 ± 5.134	106.3 ± 10.2 (*8.1*)
LS3	30.61	1.01	11.523 ± 0.030	246.470 ± 8.274	8.2	203.424 ± 6.920	138.9 ± 14.1 (*11.4*)
LS4	30.00	1.01	8.789 ± 0.062	69.240 ± 2.100	36.9	67.123 ± 2.238	29.8 ± 2.7 (*2.1*)
LS6	31.81	1.01	6.056 ± 0.037	184.232 ± 9.807	22.4	236.423 ± 12.837	146.7 ± 17.8 (*13.9*)
T1	33.57	1.01	7.825 ± 0.041	128.631 ± 10.207	19.0	120.816 ± 9.782	53.3 ± 6.5 (*5.8*)
S1	30.91	1.05	10.900 ± 0.408	37.250 ± 1.869	16.5	31.551 ± 1.909	14.2 ± 1.5 (*1.3*)
Blanks							
Cblk2880–1		1.016	37.819 ± 0.235	2.874 ± 0.257			
Cblk2880–2		1.239	22.069 ± 0.118	7.412 ± 0.432			
Cblk2937–1		0.988	20.326 ± 0.031	1.913 ± 0.185			
Cblk2938–1		1.199	16.946 ± 0.071	1.468 ± 0.107			
Cblk2007–1		1.014	97.450 ± 6.373	2.456 ± 1.261			
Cblk2007–2		1.052	87.750 ± 15.220	2.040 ± 0.459			

Cblk2007–1 and Cblk2007–2 were processed with samples LS 4 and S1; Cblk2880–1, Cblk2880–2, Cblk2937–1, Cblk2938–1were processed with the other samples.

This thinking was maintained, with multiple discussions, until the beginning of the 21st century, when new dating techniques such as TL and CRE, appeared. The early results of these new methods showed that many of the frontal moraines in the Iberian mountains actually resulted from pulses within the LGC, as in the Central System, in Sierra de Guadarrama (Palacios et al., 2012a) and in Sierra de Gredos (Palacios et al., 2011, 2012b). Moreover, evidence of moraines from the PGC were gradually being found in the Pyrenees (Lewis et al., 2009; García-Ruiz et al., 2013), in the Cantabrian Mountains (Rodríguez-Rodríguez et al., 2016), in the NW of the Peninsula (Vidal-Romaní and Fernández-Mosquera, 2006; Vidal-Romaní et al., 2015) and in Sierra Nevada (Palacios et al., 2019). In all these cases, there are two important common circumstances, which are similar to our results at Serra da Estrela. First, all the PGC moraines present ages related to HS-11, when the glaciers reached their maximum PGC extent. In fact, this coldest phase is confirmed by studies in marine sediments surrounding the Iberian Peninsula (Martrat et al., 2014; Jiménez-Amat and Zahn, 2015). Secondly, the PGC moraines that have been found, are always very close to the LGC moraines, and in some cases they even partially override them. This explains why it has been so difficult to find pre-LGC moraines in the Central System or in other Iberian mountains, although they may still occur in favourable settings, such as wide flat surfaces with frontal or lateral moraines.

The data obtained in this study suggest that in the Serra da Estrela the MIE of the LGC occurred slightly before the LGM, as elsewhere in the Central Range (Palacios et al., 2012a; Domínguez-Villar et al., 2013; Pedraza et al., 2013), in the Cantabrian mountains (Rodríguez-Rodríguez et al., 2015, 2016), in the NW Iberian mountains (Rodríguez-Rodríguez et al., 2014), and in the Sierra Nevada (Gómez-Ortiz et al., 2012, 2015).

There is multiple evidence that the deglaciation of the Serra da Estrela coincides with the onset of the B-A, as in most of the Iberian mountains (Palacios et al., 2017a). In fact, the glaciers disappeared in the Serra da Estrela around the same time than in the rest of the Central System (Palacios et al., 2011; Palacios et al., 2012a, 2012b; Carrasco et al., 2015), the Iberian Range (Fernández-Fernández et al., 2017; García-Ruiz et al., 2020), the Central Cantabrian Mountains (Rodríguez-Rodríguez et al., 2017) and the Pyrenees (Pallàs et al., 2006, 2010; Delmas, 2015; Palacios et al., 2017b; Crest et al., 2017; Tomkins et al., 2018; Andrés et al., 2019; Jomelli et al., 2020). This rapid deglaciation is fully supported by palaeoclimatic studies derived from marine and lacustrine sediments around and in the Iberian Peninsula, which indicate a sudden temperature increase up to values similar to present at the beginning of B-A (Fletcher et al., 2010a, 2010b; Moreno et al., 2014; López-Sáez et al., 2020).

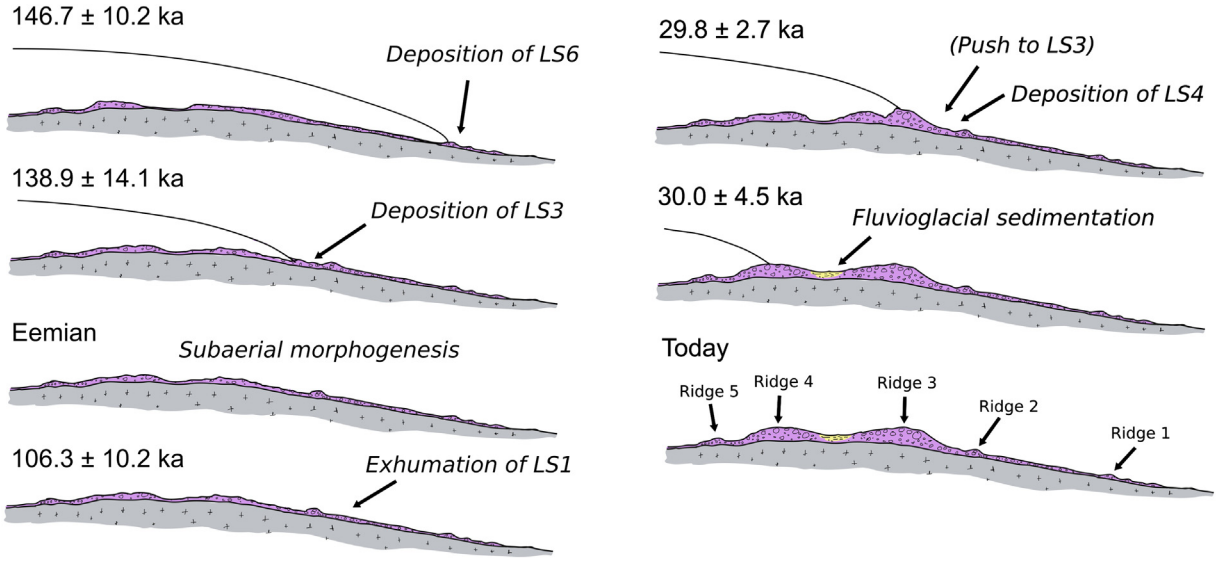

Fig. 12. Glacial evolution of the Lagoa Seca area since MIS6.

4.4. The results in the European context

The relative limited extension of glaciers during in the PGC in the Serra da Estrela, as in the rest of the Iberian Peninsula, and also in the Italian Peninsula (Kotarba et al., 2001; Giraudi et al., 2011; Giraudi and Giaccio, 2017), is in contrast to the great extension of the glaciers in the PGC, in comparison with the LGC in the Balkans (Hughes et al., 2006a, 2006b, 2007, 2010, 2011; Žebre and Stepišnik, 2014, 2015; Adamson et al., 2017; Leontaritis et al., 2020). In the Anatolia Peninsula, the presence of moraines from the PGC is limited and they are located close to the LGC moraines (Akçar et al., 2014). In the Alps, evidence of the importance of the PGC is extensive in glaciofluvial sediments (Akçar et al., 2017), but few moraines have yet been directly dated by CRE methods. One of the scarce examples is from the Jura Mountains, providing HS-11 ages (Graf et al., 2015). In most cases, the PGC advances in the Alps were slightly larger than those of the LGC (Buoncristiani and Campy, 2011).

On the other hand, the large European Pleistocene Ice Sheets showed large regional differences in the ice extent during the PGC and the LGC. The Fennoscandian Ice Sheet in Eastern Europe and Siberia during the PGC was much larger than in the LGC (Astakhov, 2013, 2018, Bachelor et al., 2019). However, in northern central Europe (Lüthgens and Böse, 2012; Lang et al., 2018), the North Sea (Reinardy et al., 2017) and the Great Britain (Gibbard and Clark, 2011), the PGC ice-sheet showed a smaller, or only slightly larger extent than that of the LGC. One possible cause for this difference may be related to the topographic and thermal effect of the Laurentian Ice Sheet, as it has grown larger in each of the last glacial cycles, on atmospheric dynamics, which yielded in the LGC a cooling effect in Europe and a relative warming in northern Russia and northwestern Siberia (Liakka et al., 2016).

The fast deglaciation of the Serra da Estrela during the B-A, as in the rest of the Iberian Peninsula, is similar to that recorded in other Mediterranean mountains by CRE dating methods. This is the case of the Atlas Mountains (Hughes et al., 2018), the Anatolian Peninsula (Köse et al., 2019; Sarıkaya et al., 2017); and the Balkans; (Ribolini et al., 2017: Styllas et al., 2018; Žebre et al., 2019). Similar evidence has been recorded in central and westhern Europe, as in the Alps (Ivy-Ochs, 2015; Moran et al., 2016), in the Tatra Mountains (Engel et al., 2014, 2015; Makos et al., 2018; Zasadni et al., 2020), in the Southern Carpathians (Gheorghiu et al., 2015) and the in British Isles (Barth et al., 2018).

5. Conclusions

Despite the limited number of samples of ^{36}Cl exposure ages of this exploratory work, the results are internally consistent, they agree with previous information from other dating methods and are consistent with geomorphological observations and current paleoclimatic knowledge. They indicate that (a) according to these criteria, it can be confirmed that the MIE in the Serra da Estrela occurred during the PGC; and (b), the glaciers reached a position very close to the PGC maximum shortly before the LGM. This is consistent with the fact that only LGC moraines have been previously detected in the Central System. So far, there is little direct dating on glacial landforms from the PGC, both in Iberia and in the rest of Europe. However, the current knowledge on the PGC is in agreement with our results from Serra da Estrela, which show a MIE at the end of the PGC, probably in coincidence with the HS-11.

The LGC MIE occurred in Serra da Estrela short before of the LGM, at ca. 30 ka, as in several other mountains in the Iberian Peninsula. The results suggest that final deglaciation at the Serra da Estrela took place at the beginning of B-A, as in other mid- altitude Iberian mountains. This was a reaction to the intense increase in temperatures that affected the Iberian Peninsula, which reached values close to modern ones. A similar process has been detected in most other Mediterranean mountains and in many glaciated areas of central and western Europe.

The outlier result in the Torre Plateau highlights the fact that CRE samples from summit plateaus may show cosmogenic inheritance and, therefore, great care must be taken when interpreting them.

Declaration of competing interest

The authors declare that they have no known competing financial interests or personal relationships that could have appeared to influence the work reported in this paper.

Acknowledgements

This research was funded by the project PR108/20-20 (Santander Bank-UCM Projects), with the help of the High Mountain Physical Geography Research Group (Complutense University of Madrid), with fieldwork and UAV surveys funded by the Fundação para a Ciência e a Tecnologia in the framework of project Altitud3 (PTDC/EAM-REM/30475/2017) and of CEG/IGOT activities under FCT IP. UIDB/00295/2020 and UIDP/00295/2020.

References

Adamson, K.R., Woodward, J.C., Hughes, P.D., Giglio, F., Del Bianco, F., 2017. Middle Pleistocene glaciation, alluvial fan development and sea-level changes in the Bay of Kotor, Montenegro. In: Hughes, P.D., Woodward, J.C. (Eds.), Quaternary Glaciation in the Mediterranean Mountains. Geological Society of London Special Publications vol. 433, pp. 193–209.

Akçar, N., Yavuz, V., Ivy-Ochs, S., Reber, R., Kubik, P.W., Zahno, C., Schluchter, C., 2014. Glacier response to the change in atmospheric circulation in the eastern Mediterranean during the Last Glacial Maximum. Quat. Geochronol. 19, 27–41.

Akçar, N., Ivy-Ochs, S., Alfimov, V., Schlunegger, F., Claude, A., Reber, R., Christl, M., Vockenhuber, C., Dehnert, A., Rahn, M., Schlüchter, C., 2017. Isochron-burial dating of glaciofluvial deposits: first results from the Swiss Alps. Earth Surf. Process. Landf. 42 (14), 2414–2425.

Andrés, N., Palacios, D., 2014. Las fases de deglaciación del Sistema central y su significado paleoclimático. In: Arnáez, J., González-Samperiz, P., Lasanta, T., Valero-Garcés, B. (Eds.), Geoecología, cambio ambiental y paisaje. CSIC, Universidad de la Rioja, Logroño, pp. 49–64.

Andrés, N., Gómez-Ortiz, A., Fernández-Fernández, J.M., Tanarro, L.M., Salvador, F., Oliva, M., Palacios, D., 2018. Timing of deglaciation and rock glacier origin in the southeastern Pyrenees: a review and new data. Boreas 47, 1050–1071. https://doi.org/10.1111/bor.12324.

Andrés, N., Gómez-Ortiz, A., Fernández-Fernández, J.M., Tanarro, L.M., Salvador, F., Oliva, M., Palacios, D., 2019. Timing of deglaciation and rock glacier origin in the southeastern Pyrenees: a review and new data. Boreas 47, 1050–1071. https://doi.org/10.1111/bor.12324.

Astakhov, V.I., 2013. Pleistocene glaciations of northern Russia – a modern view. Boreas 42, 1–24.

Astakhov, V.I., 2018. Late Quaternary glaciation of the northern Urals: a review and new observations. Boreas 47, 379–389.

Balco, G., 2011. Contributions and unrealized potential contributions of cosmogenic-nuclide exposure dating to glacier chronology, 1990–2010. Quat. Sci. Rev. 30 (1–2), 3–27.

Balco, G., Todd, C., Huybers, K., Campbell, S., Vermeulen, M., Hegland, M., Goehring, B.M., Hillebrand, T.R., 2016. Cosmogenic-nuclide exposure ages from the Pensacola Mountains adjacent to the foundation ice stream, Antarctica. Am. J. Sci. 316, 542–577. https://doi.org/10.2475/06.2016.02.

Barth, A.M., Clark, P.U., Clark, J., Roe, G.H., Marcott, S.A., McCabe, A.M., Caffee, M.W., He, F., Cuzzone, J.K., Dunlop, P., 2018. Persistent millennial-scale glacier fluctuations in Ireland between 24 ka and 10 ka. Geology 46 (2), 151–154. https://doi.org/10.1130/G39796.1.

Bentley, M.J., Fogwill, C.J., Kubik, P.W., Sugden, D.E., 2006. Geomorphological evidence and cosmogenic 10Be/26Al exposure ages for the Last Glacial Maximum and deglaciation of the Antarctic Peninsula Ice Sheet. Bull. Geol. Soc. Am. 118, 1149–1159. https://doi.org/10.1130/B25735.1.

Briner, J.P., Kaufman, D.S., Manley, W.F., Finkel, R.C., Caffee, M.W., 2005. Cosmogenic exposure dating of late Pleistocene moraine stabilization in Alaska. Geol. Soc. Am. Bull. 117 (7–8), 1108–1120.

Briner, J.P., Gosse, J.C., Bierman, P.R., 2006. Applications of cosmogenic nuclides to Laurentide Ice Sheet history and dynamics. Spec. Pap. Geol. Soc. Am. 415, 29–41. https://doi.org/10.1130/2006.2415(03).

Buoncristiani, J.-F., Campy, M., 2011. Quaternary glaciations in the French Alps and Jura. In: Ehlers, J., Gibbard, P.L., Hughes, P.D. (Eds.), Quaternary Glaciations – Extent and Chronology – A Closer Look, Developments in Quaternary Sciences. Elsevier, pp. 117–125.

Cabral, F.A.V.P., 1884. Vestígios glaciários na Serra da Estrela. Revista de Obras Públicas e Minas, Lisboa, pp. 435–459.

Carrasco, R.M., Pedraza, J., Domínguez-Villar, D., Willenbring, J.K., Villa, J., 2015. Sequence and chronology of the Cuerpo de Hombre paleoglacier (Iberian Central System) during the Last Glacial Cycle. Quat. Sci. Rev. 129, 163–177.

Clark, P.U., Dyke, A.S., Shakun, J.D., Carlson, A.E., Clark, J., Wohlfarth, B., Mitrovica, J.X., Hostetler, S.W., McCabe, A., 2009. The Last Glacial Maximum. Science 325, 710–714. https://doi.org/10.1126/science.1172873.

Crest, Y., Delmas, M., Braucher, R., Gunnell, Y., Calvet, M., Team, A.S.T.E.R., 2017. Cirques have growth spurts during deglacial and interglacial periods: evidence from ^{10}Be and ^{26}Al nuclide inventories in the central and eastern Pyrenees. Geomorphology 278, 60–77.

CRONUS-Earth Project, d. http://web1.ittc.ku.edu:8888/html/latest/topo/ (accessed in January, 2020).

Daveau, S., 1971. La glaciation de la Serra de Estrela. Finisterra 6 (11), 5–40.

Delmas, M., 2015. The last maximum ice extent and subsequent deglaciation of the Pyrenees: an overview of recent research. Cuadernos de Investigación Geográfica. 41 (2), 359–387.

Desilets, D., Zreda, M., Almasi, P.F., Elmore, D., 2006. Determination of cosmogenic Cl-36 in rocks by isotope dilution: innovations, validation and error propagation. Chem. Geol. 233, 185–195.

Domínguez-Villar, D., Carrasco, R.M., Pedraza, J., Cheng, H., Edwards, R.L., Willenbring, J.K., 2013. Early maximum extent of paleoglaciers from Mediterranean mountains during the last glaciation. Sci. Rep. 3, 2034.

Engel, Z., Braucher, R., Traczyk, A., Laetitia, L., 2014. ^{10}Be exposure age chronology of the last glaciation in the Krkonoše Mountains, Central Europe. Geomorphology 206, 107–121. https://doi.org/10.1016/j.geomorph.2013.10.003.

Engel, Z., Mentlík, P., Braucher, R., Minár, J., Léanni, L., Team, Aster, 2015. Geomorphologicalal evidence and ^{10}Be exposure ages for the Last Glacial Maximum and deglaciation of the Velká and Malá Studená dolina valleys in the High Tatra Mountains, central Europe. Quat. Sci. Rev. 124, 106–123. https://doi.org/10.1016/j.quascirev.2015.07.015.

Fernández-Fernández, J.M., Palacios, D., García-Ruiz, J.M., Andrés, N., Schimmelpfennig, I., Gómez-Villar, A., Santos González, J., Álvarez-Martínez, J., Arnáez, J., Úbeda, J., Léanni, L., ASTER Team, 2017. Chronological and geomorphologicalal investigation of fossil debris-covered glaciers in relation to deglaciation processes: a case study in the Sierra de la Demanda, northern Spain. Quat. Sci. Rev. 170, 232–249. https://doi.org/10.1016/j.quascirev.2017.06.034.

Ferreira, N., Vieira, G., 1999. Guia Geológico e Geomorfológico do Parque Natural da Serra da Estrela. ICN/IGM, Lisbon.

Fink, D., Vogt, S., Hotchkis, M., 2000. Cross-sections for ^{36}Cl from Ti at Ep=35–150 MeV: applications to in-situ exposure dating. Nucl. Instruments Methods Phys. Res. Sect. B Beam Interact. with Mater. Atoms 172, 861–866. https://doi.org/10.1016/S0168-583X(00)00200-7.

Fletcher, W.J., Sánchez Goñi, M.F., Allen, J.R.M., Cheddadi, R., Cambourieu-Nebout, N., Huntley, B., Lawson, I., Londeix, L., Magri, D., Margari, V., Muller, U.C., Naughton, F., Novenko, E., Roucoux, K., Tzedakis, P.C., 2010a. Millennial-scale variability during the last glacial in vegetation records from Europe. Quat. Sci. Rev. 29 (21—22), 2839–2864. https://doi.org/10.1016/j.quascirev.2009.11.015.

Fletcher, W.J., Sánchez-Goñi, M.F., Peyron, O., Dormoy, I., 2010b. Abrupt climate changes of the last deglaciation. Western Mediterranean forest record. Clim. Past 6, 245–264. https://doi.org/10.5194/cp-6-245-2010.

García-Ruiz, J.M., Valero-Garcés, B.L., Martí-Bono, C., González-Sampériz, P., 2003. Asynchroneity of maximum glacier advances in the central Spanish Pyrenees. J. Quat. Sci. 18, 61–72.

García-Ruiz, J.M., Moreno, A., González-Sampériz, P., Valero-Garcés, B., Martí-Bono, C., 2010. La cronología del último ciclo glaciar en las montañas del sur de Europa. Una revisión. Cuaternario y Geomorfología 24 (1–2), 35–46.

García-Ruiz, J.M., Martí-Bono, C., Peña-Monné, J.L., Sancho, C., Rhodes, E.J., Valero-Garcés, B.L., González-Sampériz, P., Moreno, A., 2013. Glacial and fluvial deposits in the Aragón Valley, Central-Western Pyrenees: chronology of the Pyrenean late Pleistocene glaciers. Geogr. Ann. 95, 15–32.

García-Ruiz, J.M., Palacios, D., González-Sampériz, P., Andrés, N., Moreno, A., Valero-Garcés, B., Gómez-Villar, A., 2016. Mountain glacier evolution in the Iberian Peninsula during the Younger Dryas. Quat. Sci. Rev. 138, 16–30.

García-Ruiz, J.M., Palacios, D., Fernández-Fernández, J.M., Andrés, N., Arnáez, J., Gómez-Villar, A., Santos-González, J., Álvarez-Martínez, J., Lana-Renault, N., Léanni, L., ASTER Team, 2020. Glacial stages in the Peña Negra valley, Iberian Range, northern Iberian Peninsula: Assessing the importance of the glacial record in small cirques in a marginal mountain area. Geomorphology 362, 107195. https://doi.org/10.1016/j.geomorph.2020.107195.

Gheorghiu, D.M., Hosu, M., Corpade, C., Xu, S., 2015. Deglaciation constraints in the Parâng Mountains, Southern Romania, using surface exposure dating. Quat. Int. 388, 156–167.

Gibbard, P.L., Clark, C.D., 2011. Pleistocene glaciation limits in Great Britain. In: Ehlers, J., Gibbard, P.L., Hughes, P.D. (Eds.), Developments in Quaternary Sciences. Vol. 15. Elsevier, Amsterdam, pp. 75–93.

Giraudi, C., Giaccio, B., 2017. The Middle Pleistocene Glaciations on the Apennines (Italy): new chronological data and preservation of the glacial record. In: Hughes, P.D., Woodward, J.C. (Eds.), Quaternary Glaciation in Mediterranean Mountains, Special Publication. Geological Society, London, pp. 161–178.

Giraudi, C., Bodrato, G., Lucchi, M.R., Cipriani, N., Villa, I.M., Giaccio, B., Zuppi, G.M., 2011. Middle and Late Pleistocene Glaciations in the Campo Felice Basin (Central Apennines, Italy). Quat. Res. 75, 219–230.

Gómez-Ortiz, A., Palacios, D., Palade, B., Vázquez-Selem, L., Salvador-Franch, F., 2012. The deglaciation of the Sierra Nevada (Southern Spain). Geomorphology 159-160, 93–105.

Gómez-Ortiz, A., Oliva, M., Palacios, D., Salvador-Franch, F., Vázquez-Selem, L., Salvà-Catarineu, M., de Andrés, N., 2015. The deglaciation of Sierra Nevada (Spain), synthesis of the knowledge and new contributions. Cuadernos de Investigación Geográfica 41 (2), 409–426.

Graf, A., Akçar, N., Ivy-Ochs, S., Strasky, S., Kubik, P.W., Christl, M., Burkhard, M., Wieler, R., Schlüchter, C., 2015. Multiple advances of Alpine glaciers into the Jura Mountains in the Northwestern Switzerland. Swiss J. Geosci. 108 (2–3), 225–238.

Hughes, P.D., Woodward, J.C., Gibbard, P.L., 2006a. Glacial history of the Mediterranean mountains. Prog. Phys. Geogr. 30, 334–364.

Hughes, P.D., Woodward, J.C., Gibbard, P.L., 2006b. Late Pleistocene glaciers and climate in the Mediterranean region. Glob. Planet. Chang. 46, 83–98.

Hughes, P.D., Woodward, J.C., Gibbard, P.L., 2007. Middle Pleistocene cold stage climates in the Mediterranean: New evidence from the glacial record. Earth Planet. Sci. Lett. 253, 50–56.

Hughes, P.D., Woodward, J.C., van Calsteren, P.C., Thomas, L.E., Adamson, K.R., 2010. Pleistocene ice caps on the coastal mountains of the Adriatic Sea. Quat. Sci. Rev. 29, 3690–3708. https://doi.org/10.1016/j.quascirev.2010.06.032.

Hughes, P.D., Woodward, J.C., van Calsteren, P.C., Thomas, L.E., 2011. The glacial history of the Dinaric Alps, Montenegro. Quat. Sci. Rev. 30, 3393–3412. https://doi.org/10.1016/j.quascirev.2011.08.016.

Hughes, P.D., Gibbard, P.L., Ehlers, J., 2013. Timing of glaciation during the last glacial cycle: evaluating the concept of a global 'Last Glacial Maximum' (LGM). Earth Sci. Rev. 125, 171–198.

Hughes, P.D., Fink, D., Rodés, Á., Fenton, C.R., Fujioka, T., 2018. Timing of Pleistocene glaciations in the High Atlas, Morocco: new ^{10}Be and ^{36}Cl exposure ages. Quat. Sci. Rev. 180, 193–213.

Ivy-Ochs, S., 2015. Glacier variations in the European Alps at the end of the last glaciation. Cuad. Investig. Geogr. 41, 295–315.

Ivy-Ochs, S., Schaller, M., 2009. Chapter 6 Examining Processes and Rates of Landscape Change with Cosmogenic Radionuclides, Radioactivity in the Environment. 16, pp. 231–294. https://doi.org/10.1016/S1569-4860(09)01606-4.

Ivy-Ochs, S., Synal, H.A., Roth, C., Schaller, M., 2004. Initial results from isotope dilution for Cl and Cl-36 measurements at the PSI/ETH Zurich AMS facility. Nucl. Instrum. Methods Phys. Res., Sect. B 223-224, 623–627.

Jiménez-Amat, P., Zahn, R., 2015. Offset timing of climate oscillations during the last two glacial-interglacial transitions connected with large-scale freshwater perturbation. Paleoceanography 30 (6), 768–788.

Jomelli, V., Chapron, E., Favier, V., Rinterknecht, V., Braucher, R., Tournier, N., Gascoin, S., Marti, R., Galop, D., Binet, S., Deschamps-Berger, C., Tissoux, H., Team, A.S.T.E.R., 2020. Glacier fluctuations during the Late Glacial and Holocene on the Ariege valley, northern slope of the Pyrenees and reconstructed climatic conditions. Mediterranean. Geosci. Rev. 1-15. https://doi.org/10.1007/s42990-020-00018-5.

Köse, O., Sarikaya, M.A., Çiner, A., Candaş, A., 2019. Late Quaternary glaciations and cosmogenic 36Cl geochronology of Mount Dedegöl, south-west Turkey. J. Quat. Sci. 34 (1), 51–63. https://doi.org/10.1002/jqs.3080.

Kotarba, A., Hercman, H., Dramis, F., 2001. On the age of Campo Imperatore glaciations, Gran Sasso Massif, Central Italy. Geogr. Fis. Din. Quat. 24, 65–69.

Lang, J., Lauer, T., Winsemann, J., 2018. New age constraints for the Saalian glaciation in northern central Europe: implications for the extent of ice sheets and related proglacial lake systems. Quat. Sci. Rev. 180, 240–259.

Lautensach, H., 1929. Eiszeitstudien in der Serra da Estrela (Portugal). Zeitschrift für Gletscherkunde 17, 324–369.

Leontaritis, A.D., Kouli, K., Pavlopoulos, K., 2020. The glacial history of Greece: a comprehensive review. Mediterranean Geoscience Reviews 2, 65–90. https://doi.org/10.1007/s42990-020-00021-w.

Lewis, C.J., McDonald, E.V., Sancho, C., Peña, J.L., Rhodes, E.J., 2009. Climatic implications of correlated Upper Pleistocene glacial and fluvial deposits on the Cinca and Gállego rivers (NE Spain) based on OSL dating and soil stratigraphy. Glob. Planet. Chang. 67, 141–152.

Liakka, J., Löfverström, M., Colleoni, F., 2016. The impact of the North American glacial topography on the evolution of the Eurasian ice sheet over the last glacial cycle. Clim. Past 12 (5), 1225–1241. https://doi.org/10.5194/cp-12-1225-2016.

López-Sáez, J.A., Carrasco, R.M., Turu, V., Ruiz-Zapata, B., Gil-García, M.J., Luelmo-Lautenschlaeger, R., Pérez-Díaz, S., Alba-Sánchez, F., Abel-Schaad, D., Ros, X., Pedraza, J., 2020. Late Glacial-early holocene vegetation and environmental changes in the western Iberian Central System inferred from a key site: the Navamuño record, Béjar range (Spain). Quat. Sci. Rev. 230, 106167. https://doi.org/10.1016/j.quascirev.2020.106167.

Lotze, F., 1962. Überpleistozane Vergletscherungen in der Valnera Gruppe (Ostliches Kantabrisches Gebirge). Neues. Jahrb. Geol. 7, 377–381.

Lüthgens, C., Böse, M., 2012. From morphostratigraphy to geochronology – on the dating of ice marginal positions. Quat. Sci. Rev. 44, 26–36.

Makos, M., Rinterknecht, V., Braucher, R., Tołoczko-Pasek, A., Arnold, M., Aumaître, G., ... Keddadouche, K., 2018. Last Glacial Maximum and Lateglacial in the Polish High Tatra Mountains-revised deglaciation chronology based on the ^{10}Be exposure age dating. Quat. Sci. Rev. 187, 130–156. https://doi.org/10.1016/j.quascirev.2018.03.006.

Marrero, S.M., Phillips, F.M., Caffee, M.W., Gosse, J.C., 2016. CRONUS-Earth cosmogenic 36Cl calibration. Quat. Geochronol. 31, 199–219. https://doi.org/10.1016/j.quageo.2015.10.002.

Martrat, B., Jimenez-Amat, P., Zahn, R., Grimalt, J.O., 2014. Similarities and dissimilarities between the last two deglaciations and interglaciations in the North Atlantic region. Quat. Sci. Rev. 99, 122–134.

Migoń, P., Vieira, G., 2014. Granite geomorphology and its geological controls, Serra da Estrela, Portugal. Geomorphology 226, 1–14. https://doi.org/10.1016/j.geomorph.2014.07.027.

Mora, C., 2010. A Synthetic Map of the Climatopes of the Serra da Estrela (Portugal), Journal of Maps, v2010, 591–608. https://doi.org/10.4113/jom.2010.1112.

Moran, A.P., Ivy-Ochs, S., Vockenhuber, C., Kerschner, H., 2016. Rock glacier development in the Northern Calcareous Alps at the Pleistocene-Holocene boundary. Geomorphology 273, 178–188.

Moreno, A., Svensson, A., Brooks, S.J., Connor, S., Engels, S., Fletcher, W., Genty, D., Heiri, O., Labuhn, I., Persoiu, A., Peyron, O., Sadori, L., Valero-Garcés, B., Wulf, S., Zanchetta, G., 2014. A compilation of Western European terrestrial records 60-8 ka BP: towards an understanding of latitudinal climatic gradients. Quat. Sci. Rev. 106, 167–185. https://doi.org/10.1016/j.quascirev.2014.06.030.

Obermaier, H., Carandell-Pericay, J., 1917. Nuevos datos acerca de la extensión del glaciarismo cuaternario en la Cordillera Central. Extracto del Bol. Soc. Esp. Hist. Nat., XVII. Madrid.

Oliva, M., Gómez Ortiz, A., Palacios, D., Salvador-Franch, F., Salvà-Catarineu, M., 2014. Environmental evolution in Sierra Nevada (South Spain) since the Last Glaciation based on multi-proxy records. Quat. Int. 353, 195–209.

Oliva, M., Palacios, D., Fernández-Fernández, J.M., Rodríguez-Rodríguez, L., García-Ruiz, J. M., Andrés, N., Carrasco, R.M., Pedraza, J., Pérez-Alberti, A., Valcárcel, M., Hughes, P. D., 2019. Late Quaternary glacial phases in the Iberian Peninsula. Earth Sci. Rev. 192, 564–600.

Oppo, D.W., McManus, J.F., Cullen, J.L., 2006. Evolution and demise of the last interglacial warmth in the subpolar North Atlantic. Quat. Sci. Rev. 25, 3268–3277.

Palacios, D., Marcos, J., Vázquez-Selem, L., 2011. Last glacial maximum and deglaciation of Sierra de Gredos, central Iberian Peninsula. Quat. Int. 233, 16–26.

Palacios, D., Andrés, N., Marcos, J., Vázquez-Selem, L., 2012a. Glacial landforms and their paleoclimatic significance in the Sierra de Guadarrama, Central Iberian Peninsula. Geomorphology 139, 67–78.

Palacios, D., Andrés, N., Marcos, J., Vázquez-Selem, L., 2012b. Maximum glacial advance and deglaciation of the Pinar Valley (Sierra de Gredos, Central Spain) and its significance in the Mediterranean context. Geomorphology 177-178, 51–61.

Palacios, D., Gómez-Ortiz, A., Andrés, N., Vázquez-Selem, L., Salvador-Franch, F., Oliva, M., 2015. Maximum extent of Late Pleistocene glaciers and last deglaciation of La Cerdanya mountains, Southeastern Pyrenees. Geomorphology. 231, 116–129.

Palacios, D., Gómez-Ortiz, A., Andrés, N., Salvador, F., Oliva, M., 2016. Timing and new geomorphologic evidence of the Last Deglaciation stages in Sierra Nevada (southern Spain). Quat. Sci. Rev. 150, 110–129.

Palacios, D., Andrés, N., Gòmez-Ortiz, A., García-Ruiz, J.M., 2017a. Evidence of glacial activity during the Oldest Dryas in the Mountain of Spain. In: Hughes, P., Woodward, J. (Eds.), Quaternary glaciation in the Mediterranean Mountains. 433. Geological Society of London, Special Publication, pp. 87–110. https://doi.org/10.1144/SP433.10.

Palacios, D., García-Ruiz, J.M., Andrés, N., Schimmelpfennig, I., Campos, N., Leanni, L., ASTER Team, 2017b. Deglaciation in the central Pyrenees during the Pleistocene-Holocene transition: timing and geomorphological significance. Quat. Sci. Rev. 162, 111–127. https://doi.org/10.1016/j.quascirev. 2017.03.007.

Palacios, D., Gómez-Ortiz, A., Alcalá-Reygosa, J., Andrés, N., Oliva, M., Tanarro, L.M., Salvador-Franch, F., Schimmelpfennig, I., Fernández-Fernández, J.M., Lénni, L., ASTER Team, 2019. The challenging application of cosmogenic dating methods in residual glacial landforms: the case of Sierra Nevada (Spain). Geomorphology 325, 103–118.

Pallàs, R., Rodés, A., Braucher, R., Carcaillet, J., Ortuño, M., Bordonau, J., Bourlès, D., Vilaplana, J.M., Masana, E., Santanach, P., 2006. Late Pleistocene and Holocene glaciation in the Pyrenees: a critical review and new evidence from 10Be exposure ages, south-central Pyrenees. Quat. Sci. Rev. 25, 2937–2963. https://doi.org/10.1016/j.quascirev.2006.04.004.

Pallàs, R., Rodés, A., Braucher, R., Bourlès, D., Delmas, M., Calvet, M., Gunnell, Y., 2010. Small, isolated glacial catchments as priority targets for cosmogenic surface exposure dating of Pleistocene climate fluctuations, southeastern Pyrenees. Geology 38 (10), 891–894. https://doi.org/10.1130/G31164.1.

Paterson, W.S.B., 1994. The Physics of Glaciers. Elsevier, London https://doi.org/10.1016/C2009-0-14802-X.

Pedraza, J., Carrasco, R.M., Domínguez-Villar, D., Villa, J., 2013. Late Pleistocene glacial evolutionary stages in the Gredos Mountains (Iberian Central system). Quat. Int. 302, 88–100.

Penck, A., 1883. La période glaciaire dans les Pyrénées. etin la Société d'Histoire Nat. Toulouse. 19 p. 200.

Penck, A., Brückner, E., 1909. Die Alpen im Eiszeitalter. Taunitz, Leipzig.

Phillips, F.M., 2003. Cosmogenic ^{36}Cl ages of Quaternary basalt flows in the Mojave Desert, California, USA. Geomorphology 53, 199–208.

Reinardy, B.T.I., Hjelstuen, B.O., Sejrup, H.P., Augedal, H., Jørstad, A., 2017. Late Pliocene-Pleistocene environments and glacial history of the northern North Sea. Quat. Sci. Rev. 158, 107–126.

Ribolini, A., Bini, M., Isola, I., Spagnolo, M., Zanchetta, G., Pellitero, R., Mechernich, S., Gromig, R., Dunai, T., Wagner, B., Milevski, I., 2017. An Oldest Dryas Glacier Expansion on Mount Pelister (Former Yugoslavian Republic of Macedonia) According to 10Be Cosmogenic Dating. https://doi.org/10.6084/m9.figshare.c.3830254.v1.

Rodríguez-Rodríguez, L., Jiménez-Sánchez, M., Domínguez-Cuesta, M.J., Rinterknecht, V., Pallàs, R., Bourlès, D., Valero-Garcés, B., 2014. A multiple dating-method approach applied to the Sanabria Lake moraine complex (NW Iberian Peninsula, SW Europe). Quat. Sci. Rev. 83, 1–10.

Rodríguez-Rodríguez, L., Jiménez Sánchez, M., Domínguez-Cuesta, M.J., Aramburu, A., 2015. Research history on glacial geomorphology and geochronology of the Cantabrian Mountains, north Iberia (43-42°N/7-2°W). Quat. Int. 364, 6–21.

Rodríguez-Rodríguez, L., Jiménez Sánchez, M., Domínguez-Cuesta, M.J., Rinterknecht, V., Pallas, R., Bourlès, D., 2016. Chronology of glaciations in the Cantabrian Mountains (NW Iberia) during the Last Glacial Cycle based on in situ-produced ^{10}Be. Quat. Sci. Rev. 138, 31–48.

Rodríguez-Rodríguez, L., Jiménez-Sánchez, M., Domínguez-Cuesta, M.J., Rinterknecht, V., Pallàs, R., ASTER Team, 2017. Timing of last deglaciation in the Cantabrian Mountains (Iberian Peninsula; North Atlantic Region) based on in situ-produced ^{10}Be exposure dating. Quat. Sci. Rev. 171, 166–181.

Rohling, E.J., Hibbert, F.D., Williams, F.H., Grant, K.M., Marino, G., Foster, G.L., Webster, J.M., 2017. Differences between the last two glacial maxima and implications for ice-sheet, δ18O, and sea-level reconstructions. Quat. Sci. Rev. 176, 1–28.

Santos, J.B., Vieira, G., Santos-González, J., Woronko, B., Redondo-Vega, J.M., 2020. Macrofabric and grain size analysis of moraines and other till deposits in the Serra da Estrela Mountains, central Portugal. Phys. Geogr. https://doi.org/10.1080/02723646.2020.1838136.

Sarıkaya, M.A., Çiner, A., Yıldırım, C., 2017. Cosmogenic ^{36}Cl glacial chronologies of the Late Quaternary glaciers on Mount Geyikdağ in the Eastern Mediterranean. Quat. Geochronol. 39, 189–204. https://doi.org/10.1016/j.quageo.2017.03.003.

Schaefer, J.M., Oberholzer, P., Zhao, Z., Ivy-Ochs, S., Wieler, R., Baur, H., Schlüchter, C., 2008. Cosmogenic beryllium-10 and neon-21 dating of late Pleistocene glaciations in Nyalam, monsoonal Himalayas. Quat. Sci. Rev. 27 (3–4), 295–311.

Schimmelpfennig, I., 2009. Cosmogenic ^{36}Cl in Ca and K rich minerals: analytical developments, production rate calibrations and cross calibration with ^{3}He and ^{21}Ne. PhD These Universite Paul Cezanne Aix-Marseille III, CEREGE. Provence, France, Aix en.

Schimmelpfennig, I., Benedetti, L., Finkel, R., Pik, R., Blard, P.H., Bourle, D., Burnard, P., Williams, A., 2009. Sources of in situ ^{36}Cl in basaltic rocks. Implications for calibration of production rates. Quat. Geochronol. 4, 441–461.

Schimmelpfennig, I., Schaefer, J.M., Putnam, A.E., Koffman, T., Benedetti, L., Ivy-Ochs, S., Team, Aster, Schulüchter, Ch., 2014. ^{36}Cl production rate from K-spallation in the European Alps (Chironico landslide, Switzerland). J. Quat. Sci. 29, 407–413.

Serrano, E., Gómez-Lende, M., González-Amuchástegui, M.J., González-García, M., González-Trueba, J.J., Pellitero, R., Rico, I., 2015. Glacial chronology, environmental changes and implications for human occupation during the upper Pleistocene in the eastern Cantabrian Mountains. Quat. Int. 364, 22–34.

Serrano, E., González-Trueba, J.J., Pellitero, R., Gómez-Lende, M., 2017. Quaternary glacial history of the Cantabrian Mountains of northern Spain: a new synthesis. Geol. Soc. Spec. Publ. 433 (1), 55–85.

Soncco, C., 2020. Cartografia de Ultra-Alta resolución Para Monitoreo Y gestión de geossítios – Estrela Geopark, Master Thesis in GIS and Territorial Modelling Applied to Planning. IGOT, University of Lisbon http://hdl.handle.net/10451/44390.

Stone, J.O., 2000. Air pressure and cosmogenic isotope production. J. Geophys. Res. 105 (B10), 23753–23759.

Stone, J.O., Allan, G.L., Fifield, L.K., Cresswell, R.G., 1996. Cosmogenic chlorine-36 from calcium spallation. Geochim. Cosmochim. Acta 60, 679–692. https://doi.org/10.1016/0016-7037(95)00429-7.

Stone, J.O., Fifield, K., Vasconcelos, P., 2005. Terrestrial chlorine-36 production from spallation of iron. Abstract of 10th International Conference on Accelerator Mass Spectrometry. September 5–10, 2005, Berkeley, USA http://llnl.confex.com/llnl/ams10/techprogram/P1397.HTM.

Styllas, M.N., Schimmelpfennig, I., Benedetti, L., Ghilardi, M., Aumaître, G., Bourlès, D., Keddadouche, K., 2018. Late-glacial and Holocene history of the northeast Mediterranean mountain glaciers-New insights from in situ-produced ^{36}Cl-based cosmic ray exposure dating of palaeo-glacier deposits on Mount Olympus, Greece. Quat. Sci. Rev. 193, 244–265.

Tomkins, M.D., Dortch, J.M., Hughes, P.D., Huck, J.J., Stimson, A.G., Delmas, M., Calvet, M., Pallàs, R., 2018. Rapid age assessment of glacial landforms in the Pyrenees using Schmidt hammer exposure dating (SHED). Quat. Res. 90 (1), 26–37. https://doi.org/10.1017/qua.2018.12.

Turu, V., Calvet, M., Bordonau, J., Gunnell, Y., Delmas, M., Vilaplana, J.M., Jalut, G., 2016. Did Pyrenean glaciers dance to the beat of global climatic events? Evidence for the Würmian sequence stratigraphy of an ice-dammed palaeolake depocentre in Andorra. In: Hughes, P.D., Woodward, J.C. (Eds.), Quaternary Glaciation in the Mediterranean Mountains, Geological Society, London, Special Publications https://doi.org/10.1144/SP433.6 (On line).

Van der Knaap, W.O., Van Leeuwen, J.F.N., 1997. Holocene vegetation successions, altitudinal vegetation zonation, and climatic change in the Serra da Estrela. Rev. Paleobot. Palynol 97, 239–285.

Vermeesch, P., 2007. CosmoCalc: an Excel add-in for cosmogenic nuclide calculations. Geochem. Geophys. Geosyst. 8, 1525–2027.

Vidal-Romaní, J.R., Fernández-Mosquera, D., 2006. Glaciarismo Pleistoceno en el NW de la peninsula Ibérica (Galicia, España-Norte de Portugal). Enseñanza de las Ciencias de la Tierra 13, 270–277.

Vidal-Romaní, J.R., Fernández-Mosquera, D., Martin, K., 2015. The glaciation of Serra de Queixa-Invernadoiro and Serra do Geres-Xurés, NW Iberia. A critical review and a cosmogenic nuclide (^{10}Be and ^{21}Ne) chronology. Cadernos Lab. Xeolóxico de Laxe Coruña 38, 25–44.

Vieira, G., 2004. Geomorfologia dos planaltos e altos vales da Serra da Estrela. Ambientes frios do Plistocénico Superior e dinâmica actual. Universidade de Lisboa PhD Thesis.

Vieira, G., 2008. Combined numerical and geomorphological reconstruction of the Serra da Estrela plateau icefield, Portugal. Geomorphology 97 (1–2), 190–207.

Vieira, G., Nieuwendam, A., Vieira, G., 2020. Glacial and Periglacial landscapes of the Serra da Estrela. In: Zêzere, J.L., Mora, C. (Eds.), Landforms and Landscapes of Portugal. Springer, pp. 185–198.

Villa, E., Stoll, H., Farias, P., Adrados, L., Edwards, R.L., Cheng, H., 2013. Age and significance of the Quaternary cemented deposits of the Duje Valley (Picos de Europa, Northern Spain). Quat. Res. 79, 1–5.

Zasadni, J., Kłapyta, P., Broś, E., Ivy-Ochs, S., Świąder, A., Christl, M., Balážovičová, L., 2020. Latest Pleistocene glacier advances and post-Younger Dryas rock glacier stabilization

in the Mt. Kriváň group, High Tatra Mountains, Slovakia. Geomorphology, 107093 https://doi.org/10.1016/j.geomorph.2020.107093.
Žebre, M., Stepišnik, U., 2014. Reconstruction of Late Pleistocene glaciers on Mount Lovćen, Montenegro. Quat. Int. 353, 225–235.
Žebre, M., Stepišnik, U., 2015. Glaciokarst landforms and processes of the Southern Dinaric Alps. Earth Surf. Process. Landf. 40, 1493–1505. https://doi.org/10.1002/esp.3731.
Žebre, M., Sarıkaya, M.A., Stepišnik, U., Yıldırım, C., Çiner, A., 2019. First ^{36}Cl cosmogenic moraine geochronology of the Dinaric mountain karst: Velež and Crvanj Mountains of Bosnia and Herzegovina. Quat. Sci. Rev. 208, 54–75. https://doi.org/10.1016/j.quascirev.2019.02.002.
Zreda, M., Enbgland, J., Phillips, F., Elmore, D., Sharma, P., 1999. Unblocking of the Nares Strait by Greenland and Ellesmere ice-sheet retreat 10,000 years ago. Nature 398, 128–142.